nature methods

Article

https://doi.org/10.1038/s41592-023-01764-8

Engineering of bidirectional, cyanobacteriochrome-based light-inducible dimers (BICYCL)s

Received: 22 March 2022

Accepted: 21 December 2022

Published online: 23 February 2023

Check for updates

Jaewan Jang[1,5], Kun Tang[2,5], Jeffrey Youn[1], Sherin McDonald[3], Hannes M. Beyer[2], Matias D. Zurbriggen[2,4] ✉, Maruti Uppalapati[3] ✉ & G. Andrew Woolley[1] ✉

Optogenetic tools for controlling protein–protein interactions (PPIs) have been developed from a small number of photosensory modules that respond to a limited selection of wavelengths. Cyanobacteriochrome (CBCR) GAF domain variants respond to an unmatched array of colors; however, their natural molecular mechanisms of action cannot easily be exploited for optogenetic control of PPIs. Here we developed bidirectional, cyanobacteriochrome-based light-inducible dimers (BICYCL)s by engineering synthetic light-dependent interactors for a red/green GAF domain. The systematic approach enables the future engineering of the broad chromatic palette of CBCRs for optogenetics use. BICYCLs are among the smallest optogenetic tools for controlling PPIs and enable either green-ON/red-OFF (BICYCL-Red) or red-ON/green-OFF (BICYCL-Green) control with up to 800-fold state selectivity. The access to green wavelengths creates new opportunities for multiplexing with existing tools. We demonstrate the utility of BICYCLs for controlling protein subcellular localization and transcriptional processes in mammalian cells and for multiplexing with existing blue-light tools.

Optogenetic control of protein–protein interactions (PPIs) is a powerful and versatile approach for regulating diverse biological processes with high spatiotemporal resolution[1,2]. State-of-the-art optogenetic strategies integrate multiple tools and reporters to address complex processes[3]. However, these efforts are limited by the range of available colors: the majority of light-inducible dimerization tools operate in the blue (420–490 nm) and, to a lesser extent, the red or far-red (620–750 nm) range of the visible spectrum (Fig. 1a)[1–7]. Red light tools (for example, PhyB/PIF) are large (>50 kDa), or not yet structurally characterized[3,5,8]. Tools that respond to green light (520–565 nm) are limited to complex, homotetramerizing cobalamin-based systems[9,10], and optoswitches responsive to other colors (for example, yellow (570–590 nm) and orange (590–620 nm)) remain undescribed. The discovery of the cyanobacteriochromes (CBCRs), photoreceptors composed of tandem arrays of GAF (cGMP-specific phosphodiesterases, adenylyl cyclases and FhlA) domains, potentially expands the color choices for optogenetic tool development. GAF domains switch between two distinct conformational states triggered by *E/Z* isomerization of the 15–16 double bond in their chromophore; one color of light causes *E* to *Z* switching while another color triggers *Z* to *E* switching. The diversity of color responses of GAF domain variants is remarkable, and spans the full visible spectrum from ultraviolet to

[1]Department of Chemistry, University of Toronto, Toronto, Ontario, Canada. [2]Institute of Synthetic Biology, Heinrich-Heine-Universität, Düsseldorf, Germany. [3]Department of Pathology and Laboratory Medicine, University of Saskatchewan, Saskatoon, Saskatchewan, Canada. [4]CEPLAS – Cluster of Excellence on Plant Science, Düsseldorf, Germany. [5]These authors contributed equally: Jaewan Jang, Kun Tang. ✉e-mail: matias.zurbriggen@uni-duesseldorf.de; maruti.uppalapati@usask.ca; andrew.woolley@utoronto.ca

https://doi.org/10.1038/s41592-023-01764-8

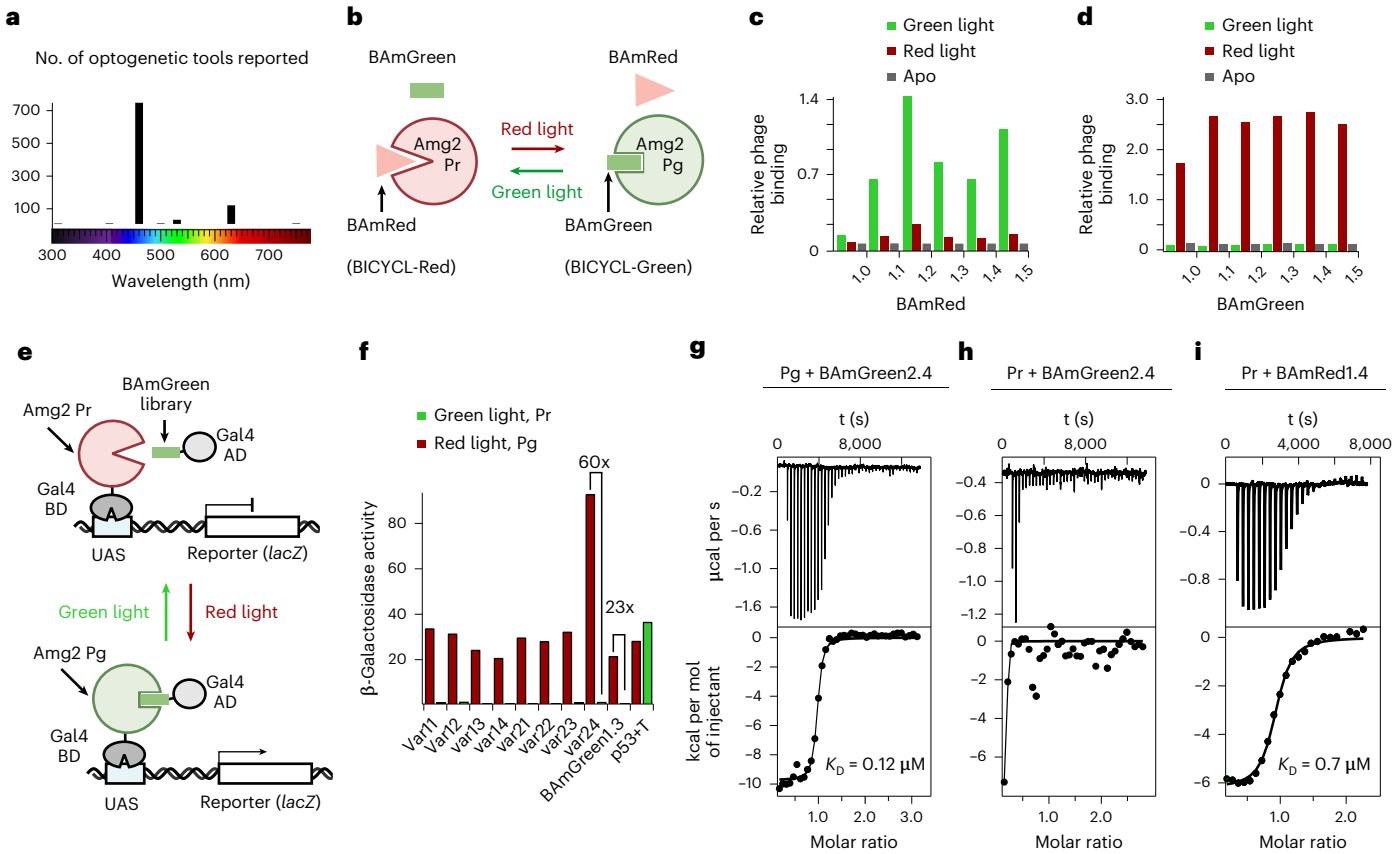

Fig. 1 | BICYCL development and characterization. a, Number of reported non-opsin optogenetic tools plotted against their associated wavelengths of activation. Data obtained from optobase.org (ref. [2]). **b**, Schematic diagram of the BICYCL-Green and BICYCL-Red systems. BICYCL-Green: red light causes Amg2 and BAmGreen to associate while green light causes dissociation. BICYCL-Red: green light causes Amg2 and BAmRed to associate while red light causes dissociation. **c**,**d**, Phage-based ELISAs of BAmGreen and BAmRed. BAmRed1.0 (**c**) was selected for binding to the ^{15Z}Pr state of Amg2. BAmRed1.1–1.5 are affinity-matured variants. BAmGreen1.0 (**d**) was selected for binding to the ^{15E}Pg state of Amg2. BAmGreen1.1–1.5 are affinity-matured variants. **e**, Schematic diagram of yeast two-hybrid selection, showing the *his3/lacZ* reporter assay used to find improved BICYCL-Green variants in yeast cells. **f**, β-Galactosidase activity of several variants after four rounds of yeast two-hybrid selection. The green/red light fold change is indicated for the best performing variant, var24. Only one trial was performed for screening purposes. **g**–**i**, ITC of BAmGreen2.4 and BAmRed1.0 binding to Amg2 in a state-selective manner. Thermograms are shown in the upper panels and calculated binding isotherms in the lower panels. BAmGreen2.4 (**g**) was titrated into a solution of Amg2 in the ^{15E}Pg state and thermogram data fitted to a 1:1 binding model to give K_D = 0.12 µM (0.063–0.18 µM) and ΔH = −9.7 ± 0.3 kcal mol^{-1}. BAmGreen2.4 (**h**) was titrated into a solution of Amg2 in the ^{15Z}Pr state and thermogram data fitted to a model in which 10% of the ^{15E}Pg state remains and the ^{15Z}Pr state is inactive. BAmRed1.4 (**i**) was titrated into a solution of Amg2 in the ^{15Z}Pr state and thermogram data fitted to a 1:1 binding model to give K_D = 0.7 µM (0.6–0.9 µM) and ΔH = −6.2 ± 0.2 kcal mol^{-1}.

far-red light[11–13]. The palette of available colors, the bi-stable behavior that enables precise spatial and temporal control, and the fact that they function as monomers without obligate oligomerization upon state switching make GAF domains the ideal components of optogenetic tools. Their small size of ~160 amino acids suits requirements for viral packaging and in vivo applications. However, no naturally occurring or engineered light-dependent binding partners for CBCRs have been discovered, limiting CBCR-based optogenetic tools to those with a predefined natural function (for example, adenylyl cyclase activity)[14,15].

Here, we describe the engineering of bidirectional, cyanobacteriochrome-based light-inducible dimers (BICYCL)s. BICYCLs consist of a CBCR GAF domain, and a binding partner identified and systematically engineered from a library of variants of the albumin-binding domain of protein G (GA domain) using phage display and yeast two-hybrid methods. The two optoswitches developed here, BICYCL-Red and BICYCL-Green (Fig. 1b), are the first CBCR-based tools that enable robust, versatile control of PPIs in vitro, in yeast and in animal cells. We demonstrate their utility for controlling subcellular protein localization and transcriptional processes, as well as their suitability for multiplexing with the existing blue-light tools LEXY, LINuS and TULIPs[16].

Results

Discovery of state-selective binders for Amg2

We chose *AM1_C0023g2*, a 190-residue, red/green GAF domain from *Acaryochloris marina*, and generated a smaller (161-residue), monomeric variant, Amg2 (Supplementary Figs. 1 and 2a)[17], by introducing an L405K mutation on the carboxy-terminal helix and truncating the amino-terminal helix. Like most CBCRs, Amg2 uses the chromophore phycocyanobilin, which can be added to cell culture, or the enzymes needed for its biosynthesis co-expressed in bacterial or animal cells[8,18].

Amg2 switches from a thermally stable, red-light-absorbing state (^{15Z}Pr) to a green-light-absorbing state (^{15E}Pg) under red light exposure, and switches in the reverse direction from ^{15E}Pg to ^{15Z}Pr with green light (Supplementary Fig. 2b). The ^{15E}Pg state slowly reverts to the ^{15Z}Pr state in darkness (half-life, 25 h at 37 °C; Supplementary Fig. 2c). We used a coat protein pVIII phage display based on the 55-residue GA domain to search for binding partners that would recognize conformational differences between the ^{15Z}Pr and ^{15E}Pg states of Amg2 (ref. [19]). Following

https://doi.org/10.1038/s41592-023-01764-8

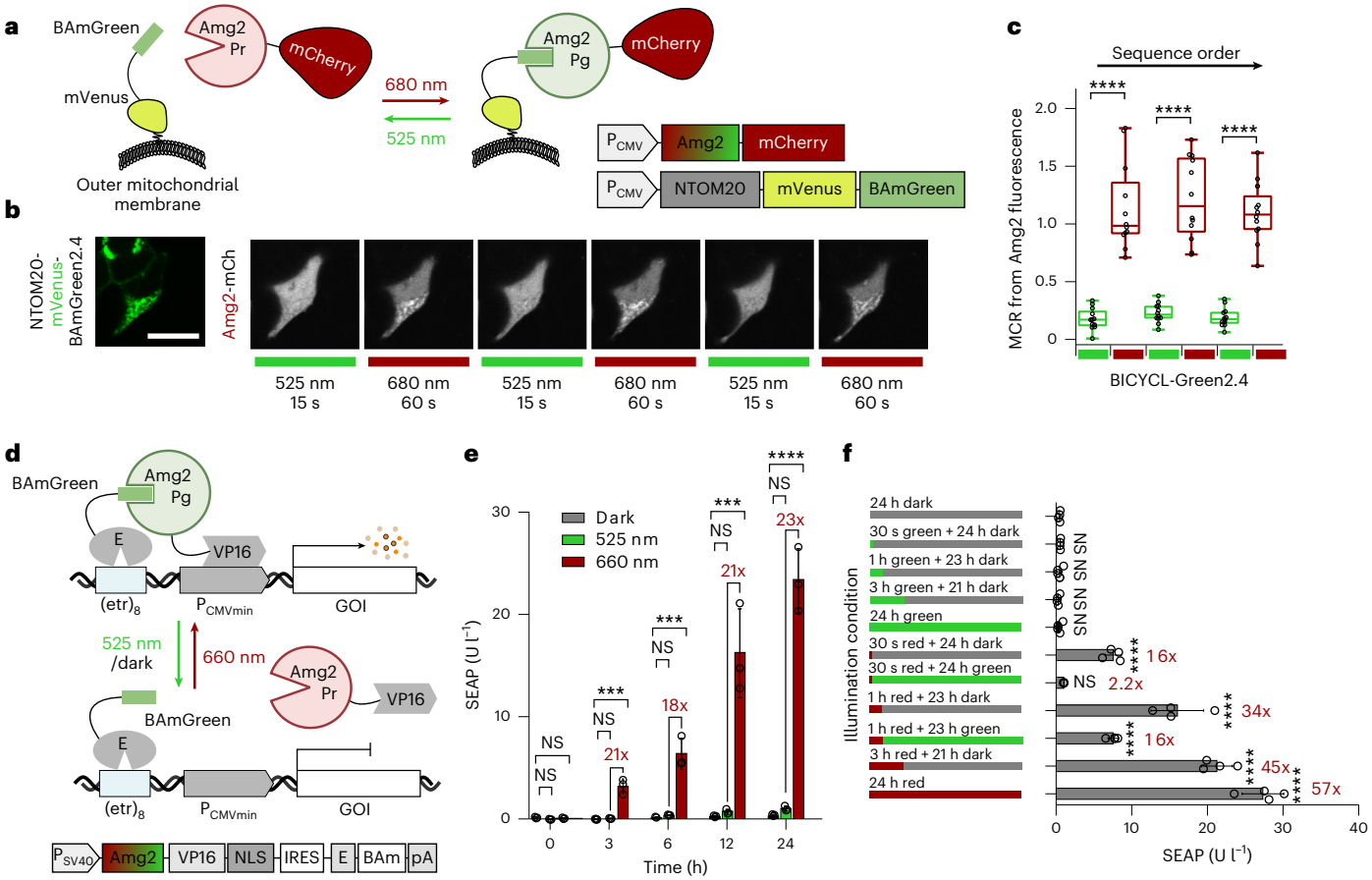

Fig. 2 | BICYCL-Green optogenetic systems in mammalian cells. **a**, Construct layout and schematic diagram of mitochondrial BAmGreen2.4 and cytoplasmic Amg2. **b**, Representative far-red fluorescence (640 nm excitation, 700 nm ± 25 nm emission) confocal images of Amg2 with NTOM20-mVenus-BAmGreen2.4 in HEK293T cells. Amg2 was cycled with alternating green (525 nm, 10 µmol m^{-2} s^{-1}, 15 s) and red (680 nm, 60 µmol m^{-2} s^{-1}, 60 s) light. Scale bar, 20 µm. **c**, Box plot of the MCR (Methods) over several red–green light cycles from **b** (left to right) ($n = 12$ cells examined in three independent experiments). ****$P < 0.0001$ (one-tailed t-test, 95% confidence interval). The center of the box indicates the median and the ends of the box indicate the 25th and 75th percentiles. The whiskers indicate the minimum and maximum. **d**, Schematic and bicistronic expression construct for BICYCL-Green-based light-induced gene expression. Amg2 was fused to the VP16 transactivator. BAmGreen was fused to the E (erythromycin repressor) DNA-binding protein, tethering it to a response construct harboring eight etr repeats (E protein operator sequence) upstream of a minimal promoter, (etr_8)-P_{CMVmin}. Red light causes Amg2 and BAmGreen to associate, inducing gene transcription. Under darkness or green light, Amg2 dissociates from BAmGreen. **e**, Dynamics of gene expression induced by BICYCL-Green. CHO-K1 cells were transiently co-transfected with the SEAP reporter and with the BICYCL-Green2.4 vector, v1 (Supplementary Fig. 15). Cells were exposed to either red light (660 nm, 20 µmol m^{-2} s^{-1}), green light (525 nm, 10 µmol m^{-2} s^{-1}), or kept in darkness for the indicated time, and SEAP levels were determined. Data are given as the mean ± s.d. of $n = 3$ independent samples. **f**, Experiment as in **e** with red and green light pulses, showing that 30 s red light exposure is sufficient to induce ~30% of the maximum transcriptional activation. Slow dark reversion (~25 h at 37°C) explains stronger induction with 1 h red + 23 h darkness than with 1 h red + 23 h green. Data are given as the mean ± s.d. of $n = 4$ independent samples. **e**,**f**, *$P < 0.05$, ***$P < 0.0002$, ****$P < 0.0001$; NS, not significant (one-way ANOVA). Source data are provided as a Source Data file. For plasmids and abbreviations, see Supplementary Table 2.

selection (Methods), we screened phage pools that displayed the libraries via the pIII coat proteins using phage ELISAs[19]. BAmRed1.0 (for 'binder of Amg2-Red state'; Fig. 1b,c) and BAmGreen1.0 (for 'binder of Amg2-Green state'; Fig. 1b, d) showed 7-fold selective ^{15Z}Pr/^{15E}Pg binding and 13-fold selective ^{15E}Pg/^{15Z}Pr binding, respectively. Neither BAm interacted with apo-Amg2. A second round of selection using new libraries based on the 1.0 versions of BAms (a soft-randomization approach[20]) identified versions 1.1–1.5 of BAmRed and BAmGreen with improved affinity and dynamic range (Fig. 1c,d, respectively).

The low OFF-state binding of BAmGreen variants encouraged us to perform another round of selection to evolve BAmGreen1.0 variants that behaved well in a cellular context. We used yeast two-hybrid selection, coupling the interaction of Amg2 and BAmGreen1.0 variants to growth in the absence of histidine, and selected binders to the ^{15E}Pg state, that is, variants surviving under red light (~10^6 transformants; Fig. 1e). Of the surviving colonies, var24 (BAmGreen2.4) had a fourfold higher signal than the positive control (T + p53), and a threefold improvement in selective binding under red versus green light when compared with BAmGreen1.3, as measured by β-galactosidase activity (Fig. 1f). Given that BAmGreen1.3, 2.4 and BAmRed1.0, 1.4 exhibited robust light-induced transcription in yeast (Supplementary Fig. 3), we characterized them further in vitro.

In vitro characterization of state-selective binders

Tested alone, all proteins appeared monomeric by size exclusion chromatography (SEC) (Supplementary Fig. 2d). Mixing BAmGreen1.3 or 2.4 with Amg2 resulted in the formation of complexes under red light (Supplementary Fig. 4a,b), while BAmRed1.0 and 1.4 formed complexes with Amg2 under green light (Supplementary Fig. 4c,d). The absence of shifts in the SEC elution volume under green light with BAmGreen1.3/2.4 (Supplementary Fig. 4a,b) and under red light with BAmRed1.0 (Supplementary Fig. 4c) indicates that the dissociation constants (K_Ds) for these

https://doi.org/10.1038/s41592-023-01764-8

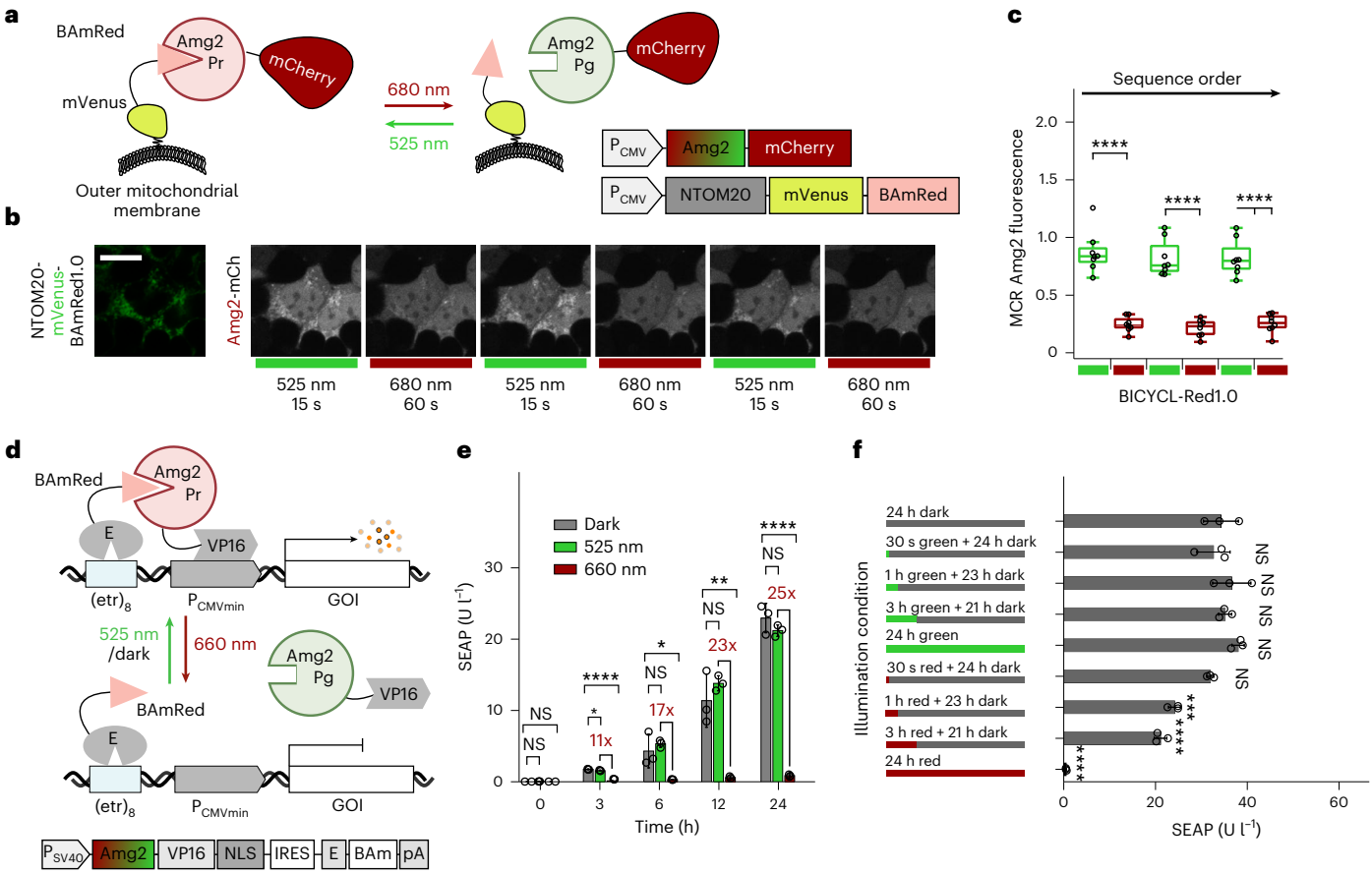

Fig. 3 | BICYCL-Red optogenetic systems in mammalian cells. a, Construct layout and schematic diagram of mitochondrial BAmRed and cytoplasmic Amg2. **b**, Representative far-red fluorescence (640 nm excitation, 700 ± 25 nm emission) confocal images of Amg2 with NTOM20-mVenus-BAmRed1.0 in HEK293T cells. Amg2 was cycled with alternating green (525 nm, 10 µmol m^{-2} s^{-1}, 15 s) and red (680 nm, 60 µmol m^{-2} s^{-1}, 60 s) light. Scale bar, 20 µm. **c**, Box plot of the MCR over several red–green light cycles (left to right) ($n = 8$ cells examined in three independent experiments). ****$P < 0.0001$ (one-tailed t-test, 95% confidence interval). The center of the box indicates the median and the ends of the box indicate the 25th and 75th percentiles. The whiskers indicate the minimum and maximum. **d**, Schematic and bicistronic expression construct for BICYCL-Red-based light-induced gene expression. Green light or darkness causes Amg2 and BAmRed to associate, inducing gene transcription. Red light converts Amg2 to the Pg state and BAmRed dissociates. **e**, SEAP expression in CHO-K1 cells transiently transfected with BICYCL-Red1.4 upon red light (660 nm, 20 µmol m^{-2} s^{-1}) or green light (525 nm, 10 µmol m^{-2} s^{-1}) exposure. Alternatively, the cells were kept in darkness for the indicated time. Data are presented as the mean ± s.d. of $n = 3$ independent samples. **f**, SEAP expression in CHO-K1 cells transiently transfected with BICYCL-Red1.4 and exposed to different green, red and dark illumination schemes. Slow dark reversion (~25 h at 37°C) causes decay of red light-induced suppression of SEAP expression. Data are presented as the mean ± s.d. of $n = 3$ independent samples. **e**,**f**, *$P < 0.05$, **$P < 0.002$, ***$P < 0.0002$, ****$P < 0.0001$; NS, not significant (one-way ANOVA). Source data are provided as a Source Data file. For plasmids and abbreviations, see Supplementary Table 2.

associations are >100 µM. The chromatogram of BAmRed1.4 indicated residual binding to Amg2 under red light (Supplementary Fig. 4d).

Next, we determined the binding affinities of the evolved photoswitches by titrating BAmGreen1.3 and 2.4 into an isothermal titration calorimetry (ITC) cell containing red-light-irradiated Amg2. The obtained data fit well to a 1:1 binding model with $K_D = 0.25$ µM and $K_D = 0.12$ µM, respectively (Fig. 1g and Supplementary Fig. 5a), while titrating green-light-irradiated Amg2 did not cause significant binding (Fig. 1h and Supplementary Fig. 5b). Together, the SEC and ITC data indicate that BAmGreen1.3 exhibits >400-fold and BAmGreen2.4 >800-fold changes in K_D in green versus red light. For BAmRed1.0 and 1.4, the ITC data also fit well to a 1:1 binding model with $K_D = 1.8$ µM and 0.7 µM, respectively (Fig. 1i and Supplementary Fig. 5c). We could further confirm BAmRed affinity values using fluorescence titrations (Supplementary Fig. 6). The results for BAmRed1.0, in combination with the SEC data, indicate a >55-fold change in K_D in red versus green light. The K_D data for all variants are summarized in Supplementary Table 1. Amg2 in combination with BAmGreen2.4, referred to as BICYCL-Green2.4, exhibits both a high affinity and a high dynamic range. Amg2 in combination with BAmRed1.0, referred to as BICYCL-Red1.0, exhibited a high dynamic range, while Amg2 in combination with BAmRed1.4, referred to as BICYCL-Red1.4, had a higher affinity.

BICYCL-Green optogenetic systems in mammalian cells

We then implemented the BICYCL systems to control protein subcellular localization and transcriptional processes in mammalian cells using standard transient transfection protocols. Figure 2 shows the performance of the BICYCL-Green optogenetic system. Holo-Amg2 can be directly visualized by its intrinsic far-red fluorescence ($\lambda_{excitation} = 640$ nm, $\lambda_{emission} = 700$ nm)[17]. BAmGreen2.4 was anchored to the mitochondrial outer membrane using an NTOM20 tag (Fig. 2a)[7]. Determining the mitochondria-to-cytoplasmic ratios (MCRs; Methods) enabled assessment of light-switchable protein binding. Under green light, Amg2 was located predominantly in the cytosol, while red light caused accumulation at the mitochondria, increasing the MCR by six-fold for at least three cycles (Fig. 2b,c). No dark reversion was observed for at least 1 hour following irradiation (Supplementary Fig. 13). We note that the excitation wavelength used for visualizing Amg2 can

https://doi.org/10.1038/s41592-023-01764-8

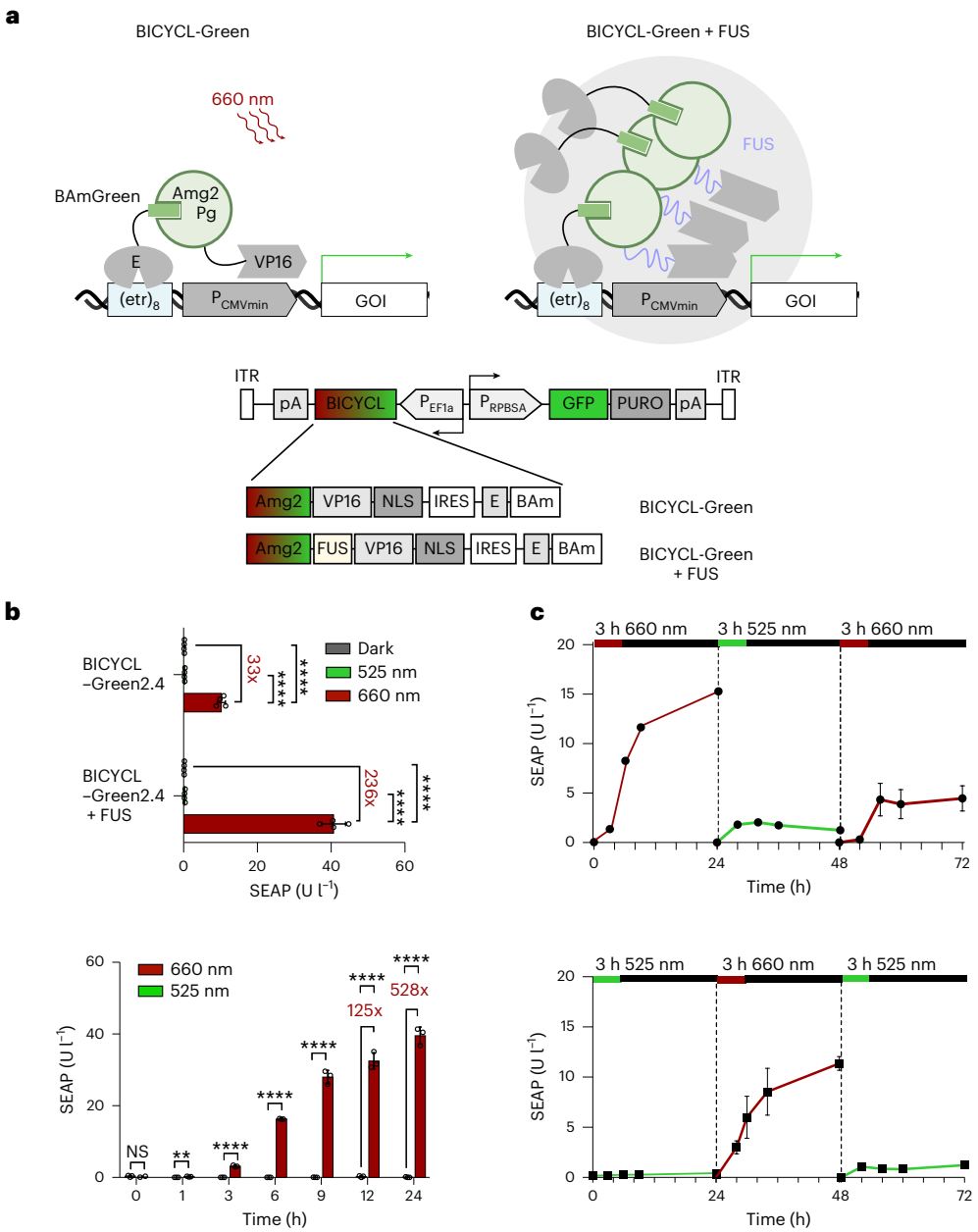

Fig. 4 | Genomically engineered BICYCL-Green gene expression cells. **a**, Schematic and construct design of BICYCL-Green gene expression cells. The bidirectional vector enables transposition of the BICYCL-Green system into the genome and fluorescence as well as antibiotic selection. Transient transfection of a matching reporter complements the optogenetic gene switch. **b**, Top: validation of the engineered cell cultures by transfection of a SEAP reporter construct. SEAP reporter levels were measured after 24 h of red light (660 nm, 20 µmol m^{-2} s^{-1}) or green light (525 nm, 10 µmol m^{-2} s^{-1}) exposure. Data are presented as the mean ± s.d. of $n = 4$ independent experiments. ****$P < 0.0001$ (one-way ANOVA). Bottom: the time dependence of SEAP expression using the BICYCL-Green2.4 (FUS) system. Data are presented as the mean ± s.d. of $n = 3$ independent samples. **$P < 0.0021$, ****$P < 0.0001$ (two-tailed unpaired t-test). **c**, Reversible control of gene expression using the genomically engineered BICYCL-Green2.4 (FUS) CHO-K1 cells. Every 24 h, the cell culture medium was replaced with a fresh phycocyanobilin-containing medium and the cells were illuminated as indicated. Data are presented as the mean ± s.d. of $n = 4$ independent samples. For transcript levels, see Supplementary Fig. 21.

cause partial ^{15Z}Pr-to-^{15E}Pg state conversion or vice versa. Re-irradiation can be used to reverse this effect after imaging (Supplementary Fig. 14). We could also observe similar reversible control capabilities with BAmGreen1.3 (Supplementary Fig. 7). BICYCL-Green switches remained functional both with N- and C-terminal fluorescent protein fusions to Amg2 (Supplementary Fig. 8).

The precise observed MCR depends, in addition to changes in binding affinity, on expression levels as well as the apo : holo ratio of the photoswitchable domain[4,21]. Given that all of the studied binders showed negligible apo-state binding (Supplementary Figs. 9–12), the fraction of apo-protein present can be assessed by comparing monomeric red fluorescent protein (tagRFP) fluorescence images, which reflect total Amg2 protein (apo + holo) present, with direct imaging of Amg2, which reflects holo-protein only. We found that the apo : holo ratio of Amg2 could be adjusted by simply increasing the concentration of phycocyanobilin (Supplementary Figs. 9–12). Alternatively, mammalian cells engineered for expression of phycocyanobilin biosynthesis genes[18] may be useful for producing predominately holo-protein.

https://doi.org/10.1038/s41592-023-01764-8

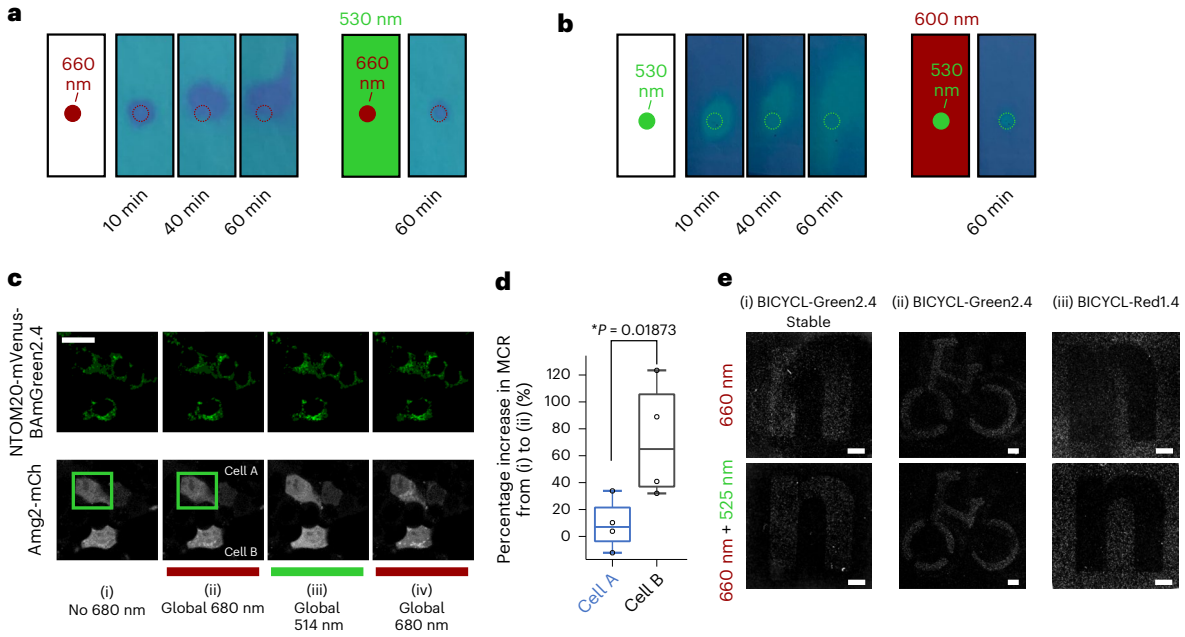

Fig. 5 | Bidirectional switching of BICYCLs for spatial optogenetic control. **a**, Images showing a solution of purified Amg2 in the Pr state (cyan) irradiated with a localized beam of 660 nm light to induce Pg state (blue) formation. Pg state protein diffuses away from the site of irradiation. Simultaneous global green light (530 nm) illumination reverts molecules leaving the beam to Pr-Amg2. **b**, Images showing a solution of purified Amg2 in the Pg state irradiated with a localized beam of 530 nm light with or without global irradiation with 660 nm light. **c**, Representative confocal images of Amg2-mCherry with NTOM20-mVenus-BAmGreen2.4 (Fig. 2a). Localized 514 nm irradiation (green box) (i) causes Amg2 to dissociate from mitochondria in that region (cell A) but neighboring areas are also affected (cell B). Simultaneous global irradiation with 680 nm light (ii) minimizes this effect. For reference, (iii) and (iv) show the effects of only global irradiation with 514 nm or 680 nm light, respectively. Scale bar, 20 µm. **d**, Box plot of the percentage change in MCR from (i) to (ii) for cell A (localized green light irradiated cell) and cell B (neighboring cell). Global 680 nm illumination helps to preserve MCR, that is, the MCR of cell B in (ii) is higher than in (i). Four independent images from four different biological replicates were analyzed ($n = 4$). *$P < 0.0332$ (one-tailed t-test, 95% confidence interval). The center of the box indicates the median, and the ends of the box indicate the 25th and 75th percentiles. The whiskers indicate the minimum and maximum. **e**, Spatial gene expression. Light-induced spatial patterning of gene expression (24 h, upper panel, 660 nm (20 µmol m^{-2} s^{-1})) was achieved by illuminating genomically engineered BICYCL-Green cells (i), or transiently transfected BICYCL-Green (ii) or BICYCL-Red (iii) cells transfected with an mCherry reporter through a photomask. Global 525 nm illumination (24 h, 0.4 µmol m^{-2} s^{-1}) sharpened the spatial pattern (lower panel). Scale bars, 5 mm. The photomask images shown were produced experimentally in at least two independent experiments. Data shown are representative. Source data are provided as a Source Data file.

To enable light-inducible gene expression by BICYCL-Green, we engineered split-transcription factor switches based on our previous work with plant phytochromes[18,22,23]. We designed different domain fusion orientations and expression vectors and assessed their behavior upon transient transfection into CHO-K1 cells (a Chinese hamster ovary cell line) using a secreted alkaline phosphatase (SEAP) reporter (Supplementary Fig. 15). The molecular design V1(Amg2-VP16-IRES-E-BAm) resulted in the best overall performance (Fig. 2d,e and Supplementary Fig. 15). Testing a range of chromophore concentrations (Supplementary Fig. 16a) suggested the optimal concentration of 40 µM phycocyanobilin, which we used in all further cell experiments. Figure 2e shows the expression of SEAP in cells exposed to red light compared with those exposed to green light or kept in darkness for different periods of time. Red light caused an up to 23-fold increase in SEAP levels while very little background expression was observed with green light exposure. Transcript levels were also measured (Supplementary Fig. 17a,c,e). We tested different illumination protocols with varying red/green/dark exposure schemes and found that as little as 30 s of red light exposure resulted in ~30% of the maximum transcriptional activation (Fig. 2f). Once activated, the BICYCL-Green system remained stable in the dark, given that SEAP levels measured after 24 h of dark incubation were approximately sevenfold higher than those measured when reverting Amg2 to the Pr state using green light to turn off expression after 30 s of red light (Fig. 2f). Note that higher expression levels are observed with longer illumination times given that measurements are affected by continuous synthesis and degradation of proteins and cell growth. Newly synthesized Amg2 will be in the Pr state if it is synthesized during a dark incubation period, and newly synthesized Amg2 interacts with BAmRed but not with BAmGreen. In vitro measurements with purified proteins showed that binding of BAmGreens slows thermal reversion of Amg2 (Supplementary Fig. 18a), indicating that there are negligible effects from thermal reversion on SEAP expression.

BICYCL-Red optogenetic systems in mammalian cells

We then characterized the BICYCL-Red optoswitches using a parallel set of constructs (Fig. 3). When BAmRed1.0 was anchored to the mitochondria, green light recruited Amg2 to the mitochondria while red light caused dissociation over several cycles (approx. fourfold; Fig. 3a–c). BAmRed1.4 behaved in a similar manner although with a lower dynamic range (approx. twofold; Supplementary Fig. 19) as expected from the in vitro K_D measurements. BICYCL-Red systems also showed full reversibility when constructed as N-terminal fusions (Supplementary Fig. 20). Control of gene expression by the BICYCL-Red system was similar to the BICYCL-Green system, with responses to green and red light reversed, as expected (Fig. 3d). Green light caused an up to 25-fold increase in SEAP levels, while very little background expression was observed with red light exposure (Fig. 3e,f). In contrast to BAmGreens, in vitro measurements indicate that BAmReds enhance thermal reversion of Amg2, although the effect is small with protein concentrations <10 µM (Supplementary Fig. 18).

The Amg2 protein has been reported to bind biliverdin in addition to phycocyanobilin[17]. Therefore, we tested optical control of subcellular protein localization and gene expression using Amg2-biliverdin with BAmRed1.0 and 1.4 (Extended Data Fig. 1). We could observe

light-inducible control of both subcellular localization and gene expression; however, the effects required the addition of exogenous biliverdin, and the performance overall was weaker than when using phycocyanobilin. Although mammalian cells commonly contain biliverdin[24], endogenous levels appear to be insufficient for chromophorylation of Amg2. Further protein engineering to improve biliverdin binding[25,26], or the use of other CBCR GAF scaffolds that selectively bind biliverdin[24], may enable the future development of biliverdin-loaded CBCR-based tools.

Genomic integration of the BICYCL optogenetic systems

Although transient transfection protocols suit basic characterization experiments of optogenetic tools, cell-to-cell variability in expression levels can alter observed degrees of switching[4,21]. Stable integration of optogenetic switches into the genome provides a more homogeneous cell population in terms of expression levels of optogenetic tools[27] and is expected to lead to more uniform degrees of switching. Stable integration is necessary for certain applications such as spatial patterning (see below), metabolic engineering[28] and in vivo cell therapy[29].

We generated a CHO-K1-derived culture harboring genomic insertions of the components constituting the BICYCL-Green optoswitch to partially alleviate the mosaicity caused by transient DNA transfection approaches, thus achieving a more uniform cell-to-cell red light control of gene expression (Fig. 4a and Supplementary Fig. 21). Transient transfection of a matching promoter DNA construct can complement these cells to produce a functional optogenetic gene switch to control the expression of any gene of interest (GOI). Two variants were designed (Fig. 4a); one was inspired by the reported transcription-enhancing effect of DropletTFs[30], in which an intrinsically disordered region of the human oncogene FUS ('fused in sarcoma'; N-terminal amino acids, 1–214) was fused to the Amg2 domain. Transfection with a SEAP reporter plasmid showed that up to 500-fold red versus green light control of gene expression was possible with this system (Fig. 4b and Supplementary Fig. 22a).

Bidirectional and spatial control capabilities of BICYCLs

BICYCLs can be switched in either direction on demand and thermal reversion is slow enough that they behave as bi-stable switches on the timescale of a few hours (Supplementary Fig. 18). Alternating cycles of 3 h red or green light with intervening periods of darkness resulted in reversibly controlled on and off switching of SEAP expression determined both at the messenger RNA and protein levels (Fig. 4c and Supplementary Fig. 22b). Bidirectional switching behavior is also seen with phytochromes and it enables improved spatial localization compared with systems such as LOV-based photoswitches, in which only dark reversion occurs[4,5,22,23,31,32]. Fig. 5a,b shows that optical control of the spatial distribution of Amg2 can be directly observed using a solution of purified protein. When Amg2 in the Pr state (which appears cyan colored) was irradiated with a localized source of red light (Fig. 5a, left panel), a blue spot appeared (due to the formation of the Pg state) and this spread over time. Simultaneous global irradiation of the solution with green light switched the Pg state protein back to the Pr state whenever it exited the zone exposed to red light, thereby enabling tighter spatial localization of the Pg state (Fig. 5a, right panel). Exactly the opposite behavior was seen with localized green light (Fig. 5b). The bidirectional switching of BICYCLs can be exploited to switch the protein activity in one cell but not in an adjacent cell. Figure 5c shows confocal microscopy images of cells in which localized green light (shown by the green rectangle) was used to cause mitochondrial dissociation of the BICYCL-Green system in a single cell (cell A). In this case, scattering of the green light also caused dissociation from mitochondria in a neighboring cell (cell B; Fig. 5c(i)), but global irradiation with red light minimized this effect (Fig. 5c(ii),d), restricting the effect of the optogenetic intervention to a smaller area.

Finally, the bidirectional switching of BICYCLs enables tight spatial control of gene expression (Fig. 5e). We used illumination masks to restrict the induction of an mCherry reporter to defined areas in cell cultures. The cultures either contained genomically integrated copies of the BICYCL-Green components for uniform cell-to-cell control of gene expression or were transiently transfected. The observed mCherry fluorescence patterns corresponded well to the projected shapes, namely, a Nature-type 'n' and a bicycle-stick figure (upper panels in Fig. 5e(i,ii)). Simultaneous global illumination with green light from one face of the culture, while projecting a red light pattern through the illumination mask from the other, yielded a sharper image than exclusive red light projection (lower panels in Fig. 5e(i,ii)), demonstrating improved spatial restriction provided by the bidirectionality of the switch. This effect was quantified using plot intensity profiles (Supplementary Fig. 23). We obtained similar results in experiments using the BICYCL-Red gene-switch, in which red light turned gene expression off in the projected areas (Fig. 5e(iii) and Supplementary Fig. 23).

Multiplexing BICYCLs with blue optogenetic tools

Optogenetic tools that respond to different colors of light provide opportunities to independently control multiple processes in living cells. To assess the compatibility of BICYCLs with existing blue-light tools, we fused Amg2 to LEXY (Fig. 6a,b) and LINuS (Supplementary Fig. 24a,b), two established optogenetic switches for blue light-inducible protein nuclear export and import, respectively[33,34]. In the dark, LEXY-tagged Amg2 predominantly localized in the nucleus, as expected, and protein that remained in the cytosol, despite the LEXY fusion, accumulated at the mitochondria upon red light irradiation (Fig. 6c). Green light reversed the mitochondrial accumulation. Blue-light irradiation caused nuclear export of LEXY-tagged Amg2 to the cytoplasm. Subsequent red- or green-light irradiation then caused association or dissociation with mitochondrial BAmGreen1.3,

Fig. 6 | Multiplexing BICYCLs with other optogenetic tools in mammalian cells. Multichromatic control of subcellular protein localization. **a**, Schematic diagram of BICYCL-Green1.3 with the blue light-inducible nuclear exporter, LEXY[34]. NES, nuclear export signal. **b**, Construct layout of the Amg2-LEXY fusion. NTOM20-mVenus-BAmGreen1.3 was constructed as in Fig. 2a. Light-dependent localization to the nucleus, cytosol and mitochondria was monitored. **c**, Far-red fluorescence microscopy images of Amg2-mCherry-LEXY, co-transfected with NTOM20-mVenus-BAmGreen1.3 in HEK293T cells. The cells were irradiated with different light conditions prior to image acquisition: 680 nm (60 µmol m^{-2} s^{-1}) and 525 nm (10 µmol m^{-2} s^{-1}) were applied continuously, while 445 nm (3 µmol m^{-2} s^{-1}) was pulsed at a 1/30 s (on/off) frequency[33,34]. Scale bar, 20 µm. **d**, Far-red fluorescence intensity of Amg2-LEXY in the nucleus, cytoplasm, and at the mitochondria was quantified and nuclear-to-cytoplasmic ratio (NCR) and MCR (Supplementary Information) were calculated for each irradiation condition ($n = 9$ cells examined in three independent experiments). $^{****}P < 0.0001$ (one-tailed t-test, 95% confidence interval). The center of the box indicates the median, and the ends of the box indicate the 25th and 75th percentiles. The whiskers indicate the minimum and maximum. **e**–**g**, Multichromatic multigene orthogonal gene expression control. **e**, Schematic diagram of the bicistronic constructs engineered for co-expression and orthogonal activity of BICYCL-Green2.4 (Amg2/BAmGreen2.4), BICYCL-Red1.4 (Amg2/BAmRed1.4), and TULIPs (LOVpep/ePDZ). **f**, Schematic diagram of orthogonal multichromatic gene expression control in a single cell. CHO-K1 cells were simultaneously transfected with constructs encoding red light-inducible SEAP (Amg2/BAmGreen2.4), green light-responsive FLuc (Amg2/BAmRed1.4) and blue light-controlled GLuc (LOVpep/ePDZ). **g**, Relative reporter levels of multigene expression using BICYCL-Green2.4, BICYCL-Red1.4 and TULIPs tools. At 24 h after transfection the culture medium was replaced with 40 µM phycocyanobilin-supplemented medium. The cells were either incubated in the dark or illuminated for 24 h prior to reporter quantification. Illumination conditions: 455 nm, 10 µmol m^{-2} s^{-1}; 525 nm, 10 µmol m^{-2} s^{-1}; 660 nm, 10 µmol m^{-2} s^{-1}. The data are presented as the mean ± s.d. of $n = 3$ independent samples. $^{**}P < 0.002$, $^{****}P < 0.0001$ (one-way ANOVA with multiple comparisons). Source data are provided as a Source Data file.

https://doi.org/10.1038/s41592-023-01764-8

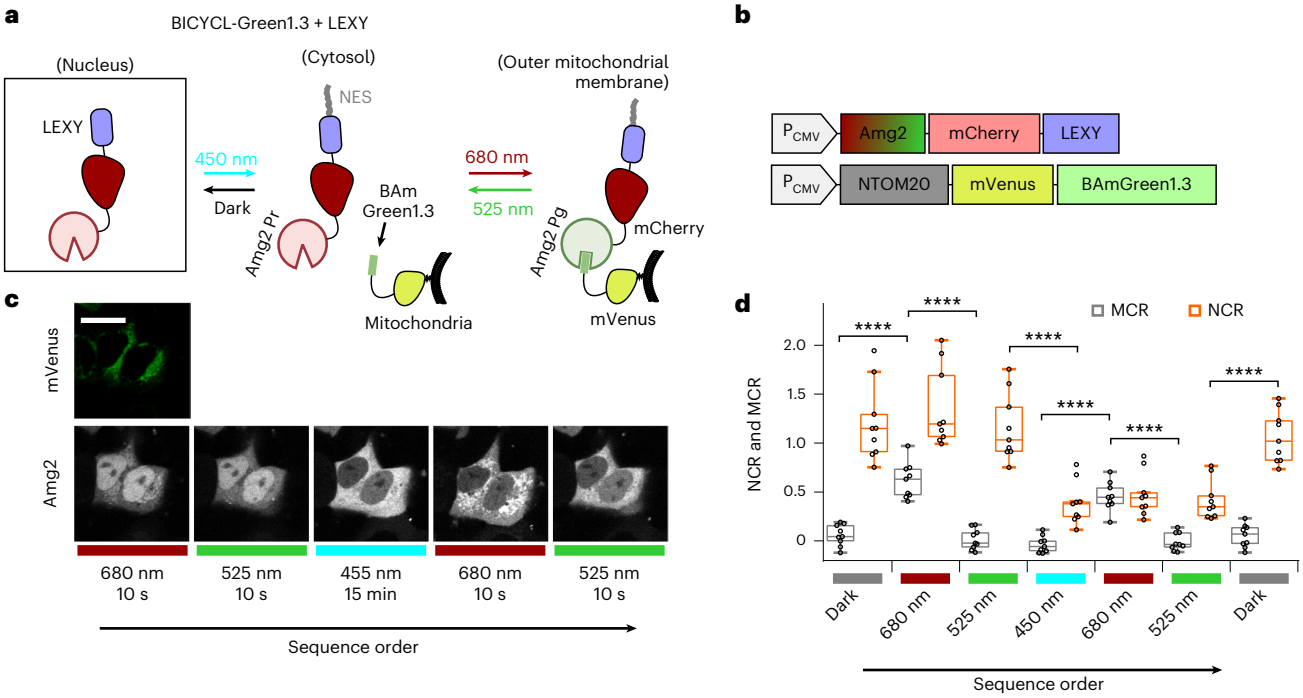

respectively, resulting in intense changes of the localization signals due to the sequential blue and red/green light-guided protein transport across multiple cellular compartments and loci. In all cases, mitochondrial-to-cytoplasmic fluorescence ratios (Methods) were independent of nuclear-to-cytoplasmic fluorescence ratios and vice versa (Fig. 6d). The LINuS-tagged BICYCL-Green1.3 system acted with reversed behavior to LEXY (Supplementary Fig. 24c,d). These rapid and reversible light-mediated recruitment tools might be applied to explore other processes, for example, the functional significance of specific organelle transport or consequences arising from light-guided repositioning inside cells[35]. Although green light did not affect LEXY or LINuS (Supplementary Fig. 25a–d), we note that the lengthy and intense blue light exposure required for LEXY/LINuS did cause some ^{15E}Pg-to-^{15Z}Pr state switching of Amg2; however, this could be overcome by simultaneous red light irradiation (Supplementary Fig. 25e–g).

To achieve independent control of the expression of multiple genes with red, green and blue light, we engineered three multiplexed systems (BICYCL-Green2.4, BICYCL-Red1.4 and blue light-activated TULIPs), six constructs in total (BICYCL-Green2.4, (tetO)7-SEAP, BICYCL-Red1.4, (etr)8-FLuc, blue light-activated TULIPs, and (UAS)5-GLuc); construct information in Supplementary Table 2) and co-transfected them into a single CHO cell culture to induce the expression of three reporters: SEAP under red light, Firefly luciferase (FLuc) under green light, and *Gaussia* luciferase (GLuc) under blue light in one cell (Fig. 6e,f). The response of this composite system was compared with the responses of all three reporters independently in darkness, under blue light (455 nm), green light (525 nm) and red light (660 nm), or with several combined light colors (Fig. 6g and Supplementary Fig. 25). As expected, red light illumination induced SEAP expression from BICYCL-Green2.4 while other colors produced low basal SEAP levels (1–2% compared with red), indicating that BAmGreen2.4 specifically binds to ^{15E}Pg-Amg2 (Fig. 6g left). With the BICYCL-Red1.4 system, FLuc expression was detected in the dark (because ^{15Z}Pr is the thermally stable state), and with green light, consistent with the selective binding of BAmRed1.4 to ^{15Z}Pr-Amg2 (Fig. 6g middle). GLuc expression was detected only under blue light (Fig. 6g, right), indicating that both BICYCL-Greens and -Reds can be used effectively in combination with blue-light transcriptional controllers. To develop a strong and tight optogenetic gene expression tool, we systematically tested a set of other multichromatic illumination conditions together with a variety of DNA-binding proteins (Supplementary Fig. 27). These data indicate that versatile, multichromatic control of gene expression can be achieved with the BICYCL-Green and BICYCL-Red systems by regulating gene dosage, chromophore concentration, light intensity and the spectral light composition.

Discussion

In summary, BICYCL-Green and BICYCL-Red systems enable light-dependent binding in a 1:1 molar ratio, with affinities between 120 nM and 2 µM for the ON state, and 10–800-fold lower affinity for the OFF state. The BICYCL-Green system enables red-ON/green-OFF and BICYCL-Red enables green-ON/red-OFF control of PPIs. Functional responses were demonstrated by exploiting light-inducible PPIs in eukaryotic cells (yeast and mammalian) to enable green- and red-light-inducible transcription and co-localization without interference from apo-protein, which is likely to be present in any heterologous system. BICYCL-Green2.4 has one of the tightest, most selective and fully reversible interactions of known light-inducible PPIs, as measured in vitro. Transfection with a SEAP reporter into a stable cell culture engineered for BICYCL-Green2.4 control of gene expression showed >500-fold red/green selectivity. The bi-stable nature of these tools also enables tight spatial and temporal control because irradiation with two different wavelengths directly controls the photoreceptor state and thus the ON and OFF state of the corresponding PPIs.

Although the bi-stable nature of these tools enables tight control, the requirement for green light may be viewed as a disadvantage for applications (for example, in vivo) that require high tissue penetrance. For this, the future engineering of GAF domains that respond to red or far-red wavelengths or that undergo red light switching with thermal relaxation may be required. Likewise, further engineering of BICYCLs to improve phycocyanobilin and/or biliverdin uptake is desirable. Substantially enhanced biliverdin uptake would enable BICYCLs to operate using endogenous biliverdin and would also red-shift the switching wavelengths.

Given that BICYCLs are based on a CBCR GAF domain (~160 residues) and a 55-residue GA three-helix bundle protein, they represent the smallest green/red optogenetic tools so far identified. In addition to the multicolor, multiplexing examples given in this work, the protein engineering pipeline we have described and the rich diversity of the CBCRs will open new directions for the design of novel multicolor optogenetic tools for in vitro and in vivo applications.

Online content

Any methods, additional references, Nature Portfolio reporting summaries, source data, extended data, supplementary information, acknowledgements, peer review information; details of author contributions and competing interests; and statements of data and code availability are available at https://doi.org/10.1038/s41592-023-01764-8.

References

1. Goglia, A. G. & Toettcher, J. E. A bright future: optogenetics to dissect the spatiotemporal control of cell behavior. *Curr. Opin. Chem. Biol.* **48**, 106–113 (2019).
2. Kolar, K., Knobloch, C., Stork, H., Znidaric, M. & Weber, W. OptoBase: a web platform for molecular optogenetics. *ACS Synth. Biol.* **7**, 1825–1828 (2018).
3. Redchuk, T. A., Omelina, E. S., Chernov, K. G. & Verkhusha, V. V. Near-infrared optogenetic pair for protein regulation and spectral multiplexing. *Nat. Chem. Biol.* **13**, 633–639 (2017).
4. Hallett, R. A., Zimmerman, S. P., Yumerefendi, H., Bear, J. E. & Kuhlman, B. Correlating in vitro and in vivo activities of light-inducible dimers: a cellular optogenetics guide. *ACS Synth. Biol.* **5**, 53–64 (2016).
5. Toettcher, J. E., Gong, D., Lim, W. A. & Weiner, O. D. Light control of plasma membrane recruitment using the Phy-PIF system. *Methods Enzymol.* **497**, 409–423 (2011).
6. Guntas, G. et al. Engineering an improved light-induced dimer (iLID) for controlling the localization and activity of signaling proteins. *Proc. Natl Acad. Sci. USA* **112**, 112–117 (2015).
7. Wang, H. et al. LOVTRAP: an optogenetic system for photoinduced protein dissociation. *Nat. Methods* **13**, 755–758 (2016).
8. Zhou, Y. et al. A small and highly sensitive red/far-red optogenetic switch for applications in mammals. *Nat. Biotechnol.* **40**, 262–272 (2022).
9. Kainrath, S., Stadler, M., Reichhart, E., Distel, M. & Janovjak, H. Green-light-induced inactivation of receptor signaling using cobalamin-binding domains. *Angew. Chem. Int. Ed. Engl.* **56**, 4608–4611 (2017).
10. Chatelle, C. et al. A green-light-responsive system for the control of transgene expression in mammalian and plant cells. *ACS Synth. Biol.* **7**, 1349–1358 (2018).
11. Fushimi, K., Ikeuchi, M. & Narikawa, R. The expanded red/green cyanobacteriochrome lineage: an evolutionary hot spot. *Photochem. Photobiol.* **93**, 903–906 (2017).
12. Rockwell, N. C., Martin, S. S. & Lagarias, J. C. Red/green cyanobacteriochromes: sensors of color and power. *Biochemistry* **51**, 9667–9677 (2012).
13. Ikeuchi, M. & Ishizuka, T. Cyanobacteriochromes: a new superfamily of tetrapyrrole-binding photoreceptors in cyanobacteria. *Photochem. Photobiol. Sci.* **7**, 1159–1167 (2008).

14. Ong, N. T. & Tabor, J. J. A miniaturized *Escherichia coli* green light sensor with high dynamic range. *Chembiochem* **19**, 1255–1258 (2018).
15. Blain-Hartung, M. et al. Cyanobacteriochrome-based photoswitchable adenylyl cyclases (cPACs) for broad spectrum light regulation of cAMP levels in cells. *J. Biol. Chem.* **293**, 8473–8483 (2018).
16. Losi, A., Gardner, K. H. & Moglich, A. Blue-light receptors for optogenetics. *Chem. Rev.* **118**, 10659–10709 (2018).
17. Fushimi, K. et al. Photoconversion and fluorescence properties of a red/green-type cyanobacteriochrome AM1_C0023g2 that binds not only phycocyanobilin but also biliverdin. *Front. Microbiol.* **7**, 588 (2016).
18. Muller, K. et al. Synthesis of phycocyanobilin in mammalian cells. *Chem. Commun.* **49**, 8970–8972 (2013).
19. Reis, J. M. et al. Discovering selective binders for photoswitchable proteins using phage display. *ACS Synth. Biol.* **7**, 2355–2364 (2018).
20. Fairbrother, W. J. et al. Novel peptides selected to bind vascular endothelial growth factor target the receptor-binding site. *Biochemistry* **37**, 17754–17764 (1998).
21. Woloschuk, R. M., Reed, P. M. M., McDonald, S., Uppalapati, M. & Woolley, G. A. Yeast two-hybrid screening of photoswitchable protein–protein interaction libraries. *J. Mol. Biol.* **432**, 3113–3126 (2020).
22. Muller, K. et al. Multi-chromatic control of mammalian gene expression and signaling. *Nucleic Acids Res.* **41**, e124 (2013).
23. Muller, K., Engesser, R., Timmer, J., Zurbriggen, M. D. & Weber, W. Orthogonal optogenetic triple-gene control in Mammalian cells. *ACS Synth. Biol.* **3**, 796–801 (2014).
24. Moreno, M. V., Rockwell, N. C., Mora, M., Fisher, A. J. & Lagarias, J. C. A far-red cyanobacteriochrome lineage specific for verdins. *Proc. Natl Acad. Sci. USA* **117**, 27962–27970 (2020).
25. Fushimi, K. et al. Rational conversion of chromophore selectivity of cyanobacteriochromes to accept mammalian intrinsic biliverdin. *Proc. Natl Acad. Sci. USA* **116**, 8301–8309 (2019).
26. Tachibana, S. R. et al. An engineered biliverdin-compatible cyanobacteriochrome enables a unique ultrafast reversible photoswitching pathway. *Int. J. Mol. Sci.* **22**, 5252 (2021).
27. Dyson, M. R. Fundamentals of expression in mammalian cells. *Adv. Exp. Med. Biol.* **896**, 217–224 (2016).
28. Guinn, M. T., Coraci, D., Guinn, L. & Balazsi, G. Reliably engineering and controlling stable optogenetic gene circuits in mammalian cells. *J. Vis. Exp.* https://doi.org/10.3791/62109 (2021).
29. Zhu, D., Johnson, H. J., Chen, J. & Schaffer, D. V. Optogenetic application to investigating cell behavior and neurological disease. *Front. Cell. Neurosci.* **16**, 811493 (2022).
30. Schneider, N. et al. Liquid–liquid phase separation of light-inducible transcription factors increases transcription activation in mammalian cells and mice. *Sci. Adv.* **7**, eabd3568 (2021).
31. Muller, K. et al. A red/far-red light-responsive bi-stable toggle switch to control gene expression in mammalian cells. *Nucleic Acids Res.* **41**, e77 (2013).
32. Levskaya, A., Weiner, O. D., Lim, W. A. & Voigt, C. A. Spatiotemporal control of cell signalling using a light-switchable protein interaction. *Nature* **461**, 997–1001 (2009).
33. Niopek, D. et al. Engineering light-inducible nuclear localization signals for precise spatiotemporal control of protein dynamics in living cells. *Nat. Commun.* **5**, 4404 (2014).
34. Niopek, D., Wehler, P., Roensch, J., Eils, R. & Di Ventura, B. Optogenetic control of nuclear protein export. *Nat. Commun.* **7**, 10624 (2016).
35. van Bergeijk, P., Adrian, M., Hoogenraad, C. C. & Kapitein, L. C. Optogenetic control of organelle transport and positioning. *Nature* **518**, 111–114 (2015).

Methods

Expression of Amg2 in *Escherichia coli*

To produce Amg2 in bacteria, the gene encoding Amg2 was subcloned into the pET24b vector containing a C-terminal poly His (6x) tag. Transformed BL21(DE3) *Escherichia coli* (New England Biolabs, C2530H) was grown at 37 °C in LB medium supplemented with 50 μg ml^{-1} kanamycin until the optical density at 600 nm (OD_{600}) reached 0.6, and expression was induced with 1 mM isopropyl-β-D-thiogalactopyranoside (IPTG). Cells were grown at 18 °C with shaking for 16 h, collected by centrifugation, and lysed by sonication in lysis buffer (50 mM phosphate, 300 mM NaCl, pH 7.5). The supernatant was separated by centrifugation and applied to a Ni-NTA column. This was washed with lysis buffer + 15 mM imidazole, and subsequently eluted with lysis buffer containing 100 mM EDTA. Eluted apo-Amg2 was dialyzed against PBS (137 mM NaCl, 3 mM KCl, 8 mM Na_2HPO_4, 1.5 mM KH_2PO_4, pH 7.2, + 5 mM 2-mercaptoethanol). 2-Mercaptoethanol was then removed using an Amicon 10K spin filter, after which the apo-protein was loaded back onto a Ni-NTA column. A twofold molar excess of purified phycocyanobilin (Frontier Scientific) in dimethylsulfoxide (DMSO) was added to the Ni-NTA column equilibrated with lysis buffer, containing the purified apo-protein and incubated overnight at 4 °C. Holo-protein was eluted using lysis buffer containing 100 mM EDTA, and then purified using a Superdex 75 10/300 GL size exclusion column (GE Healthcare) (running in PBS at 0.4 ml min^{-1}).

For phage display, Amg2 was cloned into an expression vector containing an N-terminal GST-Avi-TEV site with a C-terminal 6x His-tag[35]. AVB100 *E. coli* K12 cells (AVIDITY, EVB100) were used for in vivo biotinylation during recombinant expression of the protein. Cells were grown at 37 °C in LB medium supplemented with 100 μg ml^{-1} ampicillin until the OD_{600} reached 0.6, after which the medium was then supplemented with 50 μM D-biotin, 0.2% L-arabinose and 1 mM IPTG. Cells were grown at 18 °C for 14 h. Protein purification was carried out as described above.

Phage display-based screening

An M13 phage pVIII library based on the GA domain described previously[19] was used to find binders for the Pg or Pr state of Amg2 using the following protocol. MaxiSorp 96-well plates were coated with 5 μg ml^{-1} neutravidin in PBS (100 μl) and blocked with 200 μl PB buffer (PBS, 2 mg ml^{-1} BSA). A total of 20 μg ml^{-1} (100 μl) biotinylated apo- or holo-Amg2 (in PBS containing 2 mg ml^{-1} BSA and 0.05% Tween-20) was added and incubated for 2 h at room temperature. After the removal of unbound protein, plates were either placed under green light (525 nm, 44 μmol m^{-2} s^{-1}) to produce the Pr state, or red light (680 nm, 16 μmol m^{-2} s^{-1}) to produce the Pg state for 1 h. Apo plates were placed under ambient light conditions during this step. The GA domain phage library (~5 × 10^{12} c.f.u. ml^{-1}, 100 μl) was added to the apo plate. After incubation for 1 h at room temperature, the supernatant containing the unbound phage was transferred to either a Pg or Pr state plate for a second negative selection, followed by a positive selection on a Pr or Pg state plate, respectively, for 1 h at room temperature. Following an extensive wash (eight times), with PBS supplemented with 0.02% Tween-20, the bound phage was eluted and amplified following standard protocols[36]. The whole process was repeated twice including the apo and negative selections. The resulting library of positive clones obtained after three rounds of selection was subcloned into a pIII phagemid using *Sac*I and *Nsi*I as described previously[19]. At this point, ~100 colony forming units from each of the positive pools were screened for binding to either the Pg or the Pr state of Amg2 via a phage-based ELISA (Gen5 software for absorbance measurement)[36]. Fold-selectivities were calculated by subtracting the background binding signal from each data point.

Affinity maturation

Biased libraries were constructed in the pIII display format, based on doped oligonucleotides specific for lead clones BAmGreen1.0 and BAmRed1.0. Single-stranded DNA was isolated from each clone and used as a template for site-directed mutagenesis[37]. We used the following oligonucleotides for mutagenesis.

```
BAmGreen1.0
5'-AAGGCTGGTATCACC(N3)(N1)(N4)GAC(N2)(N2)(N4)(N2)
(N3)(N4)TTCAAC(N3)(N2)
(N4)ATCAAT(N4)(N4)(N4)GCG(N4)(N4)(N3)(N3)(N1)(N4)
GTG(N1)(N1)(N4)(N4)(N4)(N4)GTTAAC(N1)(N1)(N3)(N4)
(N4)(N4)AAGAAC(N4)(N1)(N4)ATCCTGAAAGCTCAC-3'
BAmRed1.0
5'-AAGGCTGGTATCACC(N1)(N1)(N4)GAC(N4)(N3)(N3)(N4)
(N4)(N4)TTCAAC(N3)(N1)
(N4)ATCAAT(N4)(N2)(N4)GCG(N4)(N4)(N4)(N4)(N1)(N4)
GTG(N4)(N2)(N4)(N3)(N1)(N4)GTTAAC(N3)(N4)(N4)(N4)
(N4)(N3)AAGAAC(N4)(N1)(N4)ATCCTGAAAGCTCAC-3'
Where N1 is a mix of 70% A, 10% C, 10% G, 10% T
N2 is a mix of 10% A, 70% C, 10% G, 10% T
N3 is a mix of 10% A, 10% C, 70% G, 10% T
N4 is a mix of 10% A, 10% C, 10% G, 70% T
```

Libraries were constructed using previously published protocols and this resulted in a diversity of approximately 10^9 different clones[38]. Affinity maturation selection was performed using the same protocol as for naive selection except that streptavidin was used at 2 μg ml^{-1}, and 5 μg ml^{-1} Amg2 was added to each well.

Expression of binders in *Escherichia coli*

Selected binders were subcloned from pIII phagemids into the pET24b expression vector containing a C-terminal poly His (6x) tag and transformed into BL21(DE3) cells. Cells were grown until the mid-log phase (OD_{600} ~ 0.6), and then induced with 0.75 mM IPTG and grown at 20 °C for 18 h (at 180 r.p.m.). Cells were collected, sonicated in lysis buffer (50 mM phosphate, 300 mM NaCl, pH 7.2) and centrifuged to remove cell debris. The supernatant was loaded onto a Ni-NTA column, washed with lysis buffer containing 15 mM imidazole, and eluted using lysis buffer containing 250 mM imidazole. Following elution from the Ni-NTA column, proteins were dialyzed against 1x PBS (pH 7.2) and further purified using a Superdex 75 10/300 GL size exclusion column (GE Healthcare) in PBS (137 mM NaCl, 3 mM KCl, 8 mM Na_2HPO_4, 1.5 mM KH_2PO_4, pH 7.2, 0.4 ml min^{-1} flow rate).

BAmGreen2.4 was expressed with a SUMO (small ubiquitin-like modifier) tag at the N-terminus using the same procedure as described above. Following elution of SUMO-BAmGreen2.4 from the Ni-NTA column, the protein was dialyzed against 1x PBS (pH 6.5) overnight at 4 °C. Following dialysis, the SUMO tag was removed overnight using SUMO protease (ULP1, a gift from the Kanelis laboratory) with 0.5 mM CHAPS (3-((3-cholamidopropyl) dimethylammonio)-1-propanesulfonate) added to keep BAmGreen2.4 soluble. The cleaved product was purified using a Superdex 75 10/300 GL size exclusion column in 1x PBS (pH 7.0). Protein was exchanged into 1x PBS (pH 7.2) for characterization.

Size exclusion binding assay

Amg2 (80 μM) was mixed with each binder (80 μM) in 1x PBS (pH 7.2) and injected onto a Superdex 75 10/300 GL size exclusion column (GE Healthcare, 0.4 ml min^{-1} flow rate) maintained in the dark or while both the column and sample were irradiated with either red (680 nm, 85 μmol m^{-2} s^{-1}) or green (525 nm, 44 μmol m^{-2} s^{-1}) light. Eluted proteins were collected in 0.45 ml fractions, each of which was electrophoresed on a 12.5% SDS-PAGE gel. The column was calibrated using size standards (3 mg ml^{-1} each of conalbumin, carbonic anhydrase, ribonuclease A and aprotinin).

Ultraviolet–visible light spectroscopy measurements

Ultraviolet–visible light spectra were obtained using a Perkin Elmer Lambda 35 spectrophotometer with a temperature-controlled cuvette

holder (Quantum Northwest). Amg2 samples were irradiated for 20 s with 680 nm light, and the absorbance spectra were acquired at 1 h intervals for 24 h at 37 °C. Spectra were analyzed using UV WinLab (v2.85.04, Perkin Elmer).

Fluorescence quenching binding measurements

To a fixed concentration of Amg2 (3 µM) in 1x PBS (pH 7.2), increasing amounts of BAmRed1.0 or wild-type GA domain (1–20 µM) were added, and the samples were irradiated with a 525 nm light-emitting diode (LED; to produce the Pr state) for 30 min at room temperature. Samples were excited at 628 nm and fluorescence emission was collected at 678 ± 37 nm using a BMG Labtech Clariostar plate reader and analyzed using MARS Data Analysis Software v3.33 (BMG Labtech). Fluorescence intensity data were fitted to the Morrison equation for tight binding:

$$\mathrm{I}(B_{\mathrm{tot}}) = I_{\mathrm{init}} + (I_{\mathrm{final}} - I_{\mathrm{init}})\left[\frac{(B_{\mathrm{tot}}+A_{\mathrm{tot}}+K_d)-\sqrt{(-B_{\mathrm{tot}}-A_{\mathrm{tot}}-K_d)^2-(4A_{\mathrm{tot}}B_{\mathrm{tot}})}}{2A_{\mathrm{tot}}}\right]$$

where A_{tot} = [*Amg2*] and B_{tot} = [*BAmRed*1.0].

Isothermal titration calorimetry

The ITC experiments were performed using a MicroCal VP-ITC Micro-Calorimeter. Samples were prepared as described above for SEC binding assays. Titration experiments were performed at 25 °C. The syringe contained 250 µl of the binder, BAmRed or BAmGreen, at 550 µM or 750 µM, respectively. The cell (1.4 ml) contained Amg2 (45 µM). To obtain the Pg state, samples were pre-irradiated at 680 nm. To obtain the Pr state, samples were pre-irradiated at 525 nm prior to transferral into the cell. A small amount of the undesired state was formed in each case due to a brief exposure to low-intensity white light required for loading the syringe into the instrument. All samples were equilibrated with 1x PBS, pH 7.2. Injection volumes were 10 µl for BAmRed1.0/1.4 and 5 µl for BAmGreen1.3/2.4 with a 300 s spacing between injections. Thermogram data were integrated using NITPIC[39] and binding analysis was carried out using SEDPHAT with the recommend protocols[40,41].

In vitro spatial control

Purified Amg2 was loaded onto a 1 mm quartz cuvette. One side of the cuvette was covered with tin foil with a small hole in the center. An optical fiber connected to a 660 nm LED (Thorlabs, 7.1 mW cm^{-2}) was positioned in the middle of the hole while a 530 nm LED (Thorlabs, 0.65 mW cm^{-2}) was used to globally irradiate the other side of the cuvette. The same experiment was also carried out without 530 nm irradiation. At the indicated time points (10, 20 and 60 min) a picture was taken. Alternatively, an optical fiber connected to a 530 nm LED (Thorlabs, 3.71 mW cm^{-2}) was positioned in the middle of the hole, while a 660 nm LED (Thorlabs, 0.85 mW cm^{-2}) was used to globally irradiate the other side.

Construction of yeast plasmids

The strains Y2HGOLD (*MATa*, *trp1-901*, *leu2-3*, *112*, *ura3-52*, *his3-200*, *gal4Δ*, *gal80Δ*, *LYS2::GAL1$_{UAS}$-GAL1$_{TATA}$-His3*, *GAL2$_{UAS}$-Gal2$_{TATA}$-Ade2*, *URA 3::MEL1$_{UAS}$-Mel1$_{TATA}$*, *AUR1-C MEL1*) and Y187 (*MATα*, *ura3-52*, *his3-200*, *ade2-101*, *trp-901*, *leu2-3*, *112*, *gal4Δ*, *gal80Δ*, *met-*, *URA3::GAL1$_{UAS}$-Gal-1$_{TATA}$-LacZ*, *MEL1*) were purchased from Clontech (630489). pGAL4AD-x and pGAL4BD-y plasmids were gifts from C. Tucker (Addgene plasmid 28246, RRID:Addgene_28246; Addgene plasmid 28243, RRID:Addgene_28243) as pGAL4AD-CIB1 and pGAL4BD-Cry2 (ref. [42]). The *Amg2* gene was amplified using PCR and inserted (Gibson Assembly) into either the pGAL4AD or the pGAL4BD vector by replacing a *CIB1* or *Cry2* gene, respectively. Binder constructs were also subcloned into both plasmids using the same protocol. The BAmGreen library genes from the p3 phage display affinity maturation step were amplified using PCR and inserted between the *Bgl*II and *Bam*HI restriction enzyme cut sites in the pGAL4AD vector. For the positive control, pGBKT7-p53 and pGADT7-T (Takara, Clontech) were used, while the empty vectors (pGBKT7 DNA-BD Cloning Vector and pGADT7 AD Cloning Vector, Takara, Clontech) were used for the negative control.

Yeast two-hybrid assays

Library screening. The pGAL4AD-BAmGreen library and pGAL4BD-Amg2 were transformed into Y187 and Y2HGOLD, respectively. Y2HGOLD was plated onto yeast synthetic medium lacking tryptophan (that is, dropout (DO)−W medium), while Y187 was plated onto yeast synthetic medium lacking leucine (DO−L medium). The Y187 colonies transformed with the pGAL4AD-BAmGreen library were scraped from DO−L plates and used to inoculate 10 ml YPDA medium (1% yeast extract, 2% peptone, 2% glucose, 0.02% adenine) along with a few Y2HGOLD colonies collected from the DO−W plates. After an overnight mating process (following the manufacturer's instructions), cells were plated onto triple dropout (TDO)−L/W/H medium (yeast synthetic medium lacking leucine, tryptophan and histidine) containing 20 µM phycocyanobilin and 1 mM 3-amino-1,2,4-triazole (3-AT) and grown under 680 nm light (4.6 µmol m^{-2} s^{-1}) for 3 days. Afterwards, colonies were scraped from the plate and re-plated onto TDO−L/W/H medium (+ 20 µM phycocyanobilin, 1 mM 3-AT). This process was performed four times in total. Following the fourth round, ~20 colonies were used to inoculate 5 ml double dropout (DDO)−L/W medium (yeast synthetic medium lacking leucine and tryptophan) for a β-galactosidase activity assay described in the next section.

β-Galactosidase assay. To assay light-inducible heterodimerization of Amg2/BAm constructs, Y187 and Y2HGOLD strains containing pGAL4AD-x and pGAL4BD-y, respectively, were mated in 5 ml YPDA medium overnight. Mated clones were selected on DDO−L/W medium. The DDO−L/W medium contained 2 g l^{-1} dropout medium (Bioshop; no uracil, no histidine, no leucine, no tryptophan, no adenine), 2% glucose, 50 mg l^{-1} histidine, 100 mg l^{-1} adenine hemisulfate, 20 mg l^{-1} uracil, 1.7 g l^{-1} yeast nitrogen base (Biobasic), 5 g l^{-1} ammonium sulfate (Bioshop). A single colony was picked and used to inoculate 5 ml DDO−L/W medium then grown at 30 °C for 36 h (160 r.p.m.). Following growth, cells were diluted to an OD_{600} of 0.2 in 1.2 ml DDO−L/W medium containing 10 µM phycocyanobilin (Frontier Scientific). Cultures were grown in the dark for 3 h, then grown with either red (680 nm, 1.8 µmol m^{-2} s^{-1}) or green (525 nm, 3.2 µmol m^{-2} s^{-1}) light irradiation for another 4 h. These intensities did not appear to cause any significant bleaching of phycocyanobilin in solution over this timeframe. After the 7 h growth period, 800 µl cells were collected and washed with Z-buffer (Clontech Laboratories), followed by lysis with Y Cell Lytic reagent (Sigma Aldrich). β-Galactosidase activity was measured following the protocol described in the Matchmaker Gold Yeast Two-Hybrid System (Takara, Clontech) manual using ONPG (*o*-nitrophenyl-β-D-galactopyranosidase) as a substrate. The experiment was performed in quadruplicate.

Live cell imaging

Mammalian codon-optimized Amg2 (BioBasic) with a C-terminal mCherry or N-terminal tagRFP was subcloned into pTRIEX (a gift from K. Hahn, Addgene plasmid 81041)[7] and a pLL vector (a gift from B. Kuhlman, Addgene plasmid 60415)[6] containing a cytomegalovirus promoter for mammalian cell expression. *BAm* genes were subcloned into the same vector with an N-terminal mVenus tag that contains an NTOM20 mitochondrial localization tag on its N terminus (a gift from K. Hahn, Addgene plasmid 81010)[7]. HEK293T cells (a gift from A. McGuigan, ATCC) were cultured in DMEM supplemented with 10% FBS, phenol red, streptomycin, penicillin and amphotericin. For multicolor control experiments, the *Amg2* gene was subcloned into pDN77 (LINuS, Addgene plasmid 61347, RRID:Addgene_61343) and pDN122 (LEXY, Addgene plasmid 72655, RRID:Addgene_72657) upstream of the NES (nuclear export signal) and NLS (nuclear localization signal)

tags, respectively. Cells were seeded into a four-chamber imaging plate (Labtek) and grown at 37°C (5% CO_2) for at least 24 h. Transfection of each plasmid was carried out using lipofectamine 3000 (Invitrogen) and cells were incubated at 37 °C (5% CO_2) for a further 24 h prior to imaging. Approximately 4 h prior to imaging, 40 µM phycocyanobilin in DMSO (0.3% final [DMSO]) was added to each well and replaced with fresh DMEM immediately before imaging. For imaging experiments with biliverdin, 40 µM biliverdin (Frontier Scientific) was added 1 h following transfection. Cells were incubated for at least 24 h, then replaced with fresh DMEM for imaging.

Imaging was carried out using a Nikon A1R resonant confocal microscope with an Apo ×60 oil λS differential interference contrast N2 objective lens, numerical aperture 1.40. mVenus underwent excitation with a 488 nm laser (20 mW) and emission was monitored at 585/35 nm, while tagRFP/mCherry excitation involved a 561 nm laser (20 mW) and emission was monitored at 595/50 nm. A 640 nm laser (16% intensity) was used to excite Amg2 and its emission was collected at 700/50 nm. For co-localization experiments, the Pr and Pg states were obtained by irradiation with a 525 nm laser (10 µmol m^{-2} s^{-1} for 15 s) or 680 nm (60 µmol m^{-2} s^{-1} for 1 min) using a ThorLabs LED. For LINuS/LEXY experiments, a 445 nm laser (20 mW, 4% intensity) was pulsed for 1 s every 30 s for 15 min. For the biliverdin experiments, cells were dark adapted for at least 30 min prior to acquisition of the dark (Pfr) state, while irradiation with a 735 nm LED (0.5 µmol m^{-2} s^{-1}) was used to produce the light (Po) state.

The MCRs of fluorescence intensity were calculated as described[4]. A mitochondrial mask based on the NTOM20-mVenus-BAm binder image was created using the threshold function in ImageJ (v1.53a). A cytoplasmic region of interest was selected outside of this mitochondrial mask. Both the mitochondrial and cytoplasmic fluorescence were averaged by dividing by the number of pixels. As noted by Hallett et al.[4] the measured mitochondrial fluorescence has contributions from the cytoplasmic fluorescence above and below the mitochondria. Thus, the true mitochondrial fluorescence was calculated by subtracting cytoplasmic fluorescence from the measured mitochondrial fluorescence[4]. MCR was calculated by dividing the true mitochondrial fluorescence by the cytoplasmic fluorescence.

For single-cell control experiments, a small region of interest was assigned to one cell. The region of interest was pulsed with a 514 nm laser (20 mW) at 0.05–0.2% intensity for 20 s with or without 680 nm Thorlab LED (60 µmol m^{-2} s^{-1}) global irradiation. Far-red fluorescence for Amg2 and mVenus fluorescence was obtained as above.

Gene expression in CHO cells

The plasmids used for transient transfection were cloned with AQUA[43] or T4 ligation and detailed information is in Supplementary Table 2. Approximately 50,000 CHO-K1 cells (DSMZ, ACC 110) per well in Ham's F12 Medium (PAN Biotech) supplemented with 125 U ml^{-1} penicillin, 125 U ml^{-1} streptomycin, and 10% FBS (PAN Biotech, cat. no. P30-3602) were seeded onto 24-well plates. The next day, 750 ng DNA-mix was transfected in equimolar plasmid amounts (w/w) using polyethylenimine (Polysciences Inc. Europe). The medium was exchanged 4 h after transfection and cells were cultured overnight in the dark. At 24 h after the transfection, the medium was replaced 1 h prior to illumination with a pre-warmed medium additionally supplemented with phycocyanobilin (Frontier Specialty Chemicals, cat. no. P14137; Sirius Fine Chemicals, SC-1800) at a concentration of 40 µM if not indicated otherwise. The cells were then illuminated with light for indicated time periods or kept in the dark. Blue (455 nm), green (525 nm) and red (660 nm) illuminations were performed using custom-made LED arrays (fluence is given in the figure legends). For kinetic experiments, cells were continuously illuminated with 660 nm (20 µmol m^{-2} s^{-1}) or 525 nm (10 µmol m^{-2} s^{-1}) light for the indicated time or kept in darkness as a control. For BICYCL-biliverdin-mediated gene expression experiments, CHO-K1 cells were seeded as above, and transiently co-transfected with BICYCLs and the SEAP reporter. At 24 h after transfection the cells were changed into Hams medium with 40 µM biliverdin (Biliverdin hydrochloride, ChemCruz, sc-263030, dissolved in DMSO) and exposed to either 590 nm (20 µmol m^{-2} s^{-1}), or 700 nm (20 µmol m^{-2} s^{-1}) for 24 h.

For the qRT-PCR experiments, RNA was isolated using the NucleoSpin RNA Plus Kit (Macherey Nagel). The extracted RNA was adjusted to a final concentration of 20 ng $µl^{-1}$ and converted into complementary DNA using the LunaScript RT SuperMix Kit (NEB). qPCR experiments were conducted using the Luna Universal Probe qPCR Master Mix (NEB) with 500 ng cDNA per sample in triplicate reactions. OneStep Plus Real-Time PCR system (Applied Biosystems) or qTOWER3 real-time PCR (Analytik Jena AG) was used with the following cycling conditions: 95 °C for 10 min for initial denaturation followed by 40 cycles of (95 °C for 15 s, 60 °C for 60 s). The raw data were analyzed using the LinRegPCR program[44]. Normalized expression of the transcript level was then calculated using GAPDH as the reference. Reporter SEAP and GLuc levels were quantified in the cell culture medium, and FLuc was quantified in cell lysates, as detailed before[22].

Gene expression in stable CHO cells

Construction of stable cell lines. The Sleeping Beauty (SB) SB100X transposase system was used for genome engineering[45,46]. BICYCL-Green systems were engineered into the optimized SB-compatible plasmid pSBbi-GP (a gift from E. Kowarz, Addgene plasmid 60511, RRID:Addgene_60511)[46] via AQUA cloning[43]. A total of 3 µg pKT912 (ITR-PEF1a-Amg2-VP16-IRES-E-BAmGreen2.4-pA::RPBSA-GFP-2A-Puro-pA-ITR) or pKT914 (ITR-PEF1a-Amg2-FUS-VP16-IRES-E-BAmGreen2.4-pA::RPBSA-GFP-2A-Puro-pA-ITR) were co-transfected into CHO-K1 cells with 0.75 µg of the SB transposase expression vector (a gift from Z. Izsvak, Addgene plasmid 34879, RRID:Addgene_34879)[45], followed by selection with puromycin (10 µg ml^{-1}) for 2 weeks.

Reversibility of gene expression. Stable cells containing the FUS-modified BICYCL-Green photoswitch were transfected with a SEAP reporter plasmid (pKM081) as described above. At 24 h after transfection, the cells were illuminated with red light (660 nm, 20 µmol m^{-2} s^{-1}) or green light (525 nm, 10 µmol m^{-2} s^{-1}) for 3 h and then incubated in the dark for another 21 h. After each 24 h cycle the medium was replaced with fresh medium supplemented with 40 µM phycocyanobilin, and the cells were again illuminated for 3 h. Every 24 h, the illumination conditions were swapped with respect to the previous cycle (660 nm–525 nm–660 nm, or 525 nm–660 nm–525 nm). At the indicated time points, SEAP production was quantified in the supernatant, and cells were trypsinized for RT-qPCR.

Light-induced pattern formation with photomasks. For photomask experiments, the mCherry reporter plasmid pKM269 was transfected into BICYCL-Green stable cells (Fig. 5e(i)); for transient transfection, pKT138 was co-transfected with BICYCL (BICYCL-Green: pKT215, Fig. 5e(ii); BICYCL-Red, pKT214, Fig. 5e(iii)) into CHO-K1 cells. At 24 h after transfection, the medium was exchanged with a fresh medium containing 40 µM phycocyanobilin. The cells were exposed to red light (660 nm, 20 µmol m^{-2} s^{-1}) from below through a photomask, and green light (525 nm, 0.4 µmol m^{-2} s^{-1}) from above for 24 h. Photomasks were created with Fusion360 and 3D-printed using black filament (PRUSA). The fluorescence images are stitched tiles acquired using a CFI Plan Apochromat λD ×4 Nikon objective (NA 0.4) with an epifluorescence microscope (Nikon Ti2; mCherry excitation 578/21 nm, emission 641/75 nm; green fluorescent protein (GFP) excitation 470/40 nm, emission 525/50 nm). Tiles were corrected for shading using the Fiji[47] and the BaSiC plugin[48], and then stitched using the Grid/Collection stitching plugin. The stitched images were downscaled on average to 2.5% of their original size in Fiji and adjusted in the same brightness and

contrast for each group with or without green light. The final results were visualized in OMERO[49].

Reporting summary

Further information on research design is available in the Nature Portfolio Reporting Summary linked to this article.

Data availability

All data associated with this study are present in the article and the Supplementary Information. Source data are provided with this paper.

References

36. Fellouse, F. A. & Sidhu, S. S. in *Making and Using Antibodies: A Practical Handbook* (eds Howard, G. C. & Kaser, M. R.) Ch. 8 (CRC Press, 2007).
37. Kunkel, T. A. Rapid and efficient site-specific mutagenesis without phenotypic selection. *Proc. Natl Acad. Sci. USA* **82**, 488–492 (1985).
38. Chen, G. & Sidhu, S. S. Design and generation of synthetic antibody libraries for phage display. *Methods Mol. Biol.* **1131**, 113–131 (2014).
39. Keller, S. et al. High-precision isothermal titration calorimetry with automated peak-shape analysis. *Anal. Chem.* **84**, 5066–5073 (2012).
40. Brautigam, C. A., Zhao, H., Vargas, C., Keller, S. & Schuck, P. Integration and global analysis of isothermal titration calorimetry data for studying macromolecular interactions. *Nat. Protoc.* **11**, 882–894 (2016).
41. Zhao, H., Piszczek, G. & Schuck, P. SEDPHAT: a platform for global ITC analysis and global multi-method analysis of molecular interactions. *Methods* **76**, 137–148 (2015).
42. Kennedy, M. J. et al. Rapid blue-light-mediated induction of protein interactions in living cells. *Nat. Methods* **7**, 973–975 (2010).
43. Beyer, H. M. et al. AQUA cloning: a versatile and simple enzyme-free cloning approach. *PLoS ONE* **10**, e0137652 (2015).
44. Ruijter, J. M. et al. Amplification efficiency: linking baseline and bias in the analysis of quantitative PCR data. *Nucleic Acids Res.* **37**, e45 (2009).
45. Mates, L. et al. Molecular evolution of a novel hyperactive Sleeping Beauty transposase enables robust stable gene transfer in vertebrates. *Nat. Genet.* **41**, 753–761 (2009).
46. Kowarz, E., Loscher, D. & Marschalek, R. Optimized Sleeping Beauty transposons rapidly generate stable transgenic cell lines. *Biotechnol. J.* **10**, 647–653 (2015).
47. Schindelin, J. et al. Fiji: an open-source platform for biological-image analysis. *Nat. Methods* **9**, 676–682 (2012).
48. Peng, T. et al. A BaSiC tool for background and shading correction of optical microscopy images. *Nat. Commun.* **8**, 14836 (2017).
49. Allan, C. et al. OMERO: flexible, model-driven data management for experimental biology. *Nat. Methods* **9**, 245–253 (2012).

Acknowledgements

This work was supported by Discovery grants from the Natural Sciences and Engineering Research Council of Canada (grant RGPIN-174255 to G.A.W.; grant RGPIN-06195 to M.U.) and the German Research Foundation (DFG) (grant ZU259/2-1 to M.D.Z., Collaborative Research Center 1208 project no. 267205415, NEXTplant GRK2466 and under Germany's Excellence Strategy CEPLAS – EXC-2048/1 – Project ID 390686111 to M.D.Z.), Human Frontiers Scientific Program (HFSP RGY0063/2017 and HFSP RGP0067/2021to M.D.Z.) and the European Commission – Research Executive Agency (H2020 Future and Emerging Technologies (FET-Open) Project ID 801041 CyGenTiG to K.T., H.M.B. and M.D.Z.). H.M.B. was supported by the 'Freigeist' fellowship of the Volkswagen Foundation. We thank W. Houry (University of Toronto) for access to equipment, S. Kuschel (University of Düsseldorf) for technical assistance, T. Boissonnet for helping with image processing (University of Düsseldorf) and W. Weber (University of Freiburg) for the gift of IDR (intrinsically disordered region) plasmids. We also thank L. Koch, C. Diehl and U. Urquiza (University of Düsseldorf) and especially A. Jaikaran (University of Toronto) for careful reading and their suggestions to improve the paper.

Author contributions

J.J., K.T., M.U., M.D.Z. and G.A.W. developed the concepts and designed the experiments. J.J., S.M. and M.U. designed and carried out the phage display experiments. J.J. carried out all protein expression, purification and in vitro analyses. J.J. designed, carried out and analyzed protein subcellular localization experiments. K.T. designed, carried out and analyzed all mammalian gene expression experiments. J.Y. purified the BAmGreen2.4 protein. H.M.B. and K.T. engineered stable cell lines, and designed and performed spatial expression patterning. G.A.W., M.U. and M.D.Z. supervised the project. J.J., K.T., M.U., M.D.Z. and G.A.W. wrote the paper. All authors contributed to the editing, and read the final version of the paper.

Competing interests

The authors declare no competing interests.

Additional information

Extended data are available for this paper at https://doi.org/10.1038/s41592-023-01764-8.

Supplementary information The online version contains supplementary material available at https://doi.org/10.1038/s41592-023-01764-8.

Correspondence and requests for materials should be addressed to Matias D. Zurbriggen, Maruti Uppalapati or G. Andrew Woolley.

Peer review information *Nature Methods* thanks J. Clark Lagarias, Matthieu Sainlos and the other, anonymous, reviewer(s) for their contribution to the peer review of this work. Peer reviewer reports are available. Primary Handling Editor: Rita Strack, in collaboration with the *Nature Methods* team.

https://doi.org/10.1038/s41592-023-01764-8

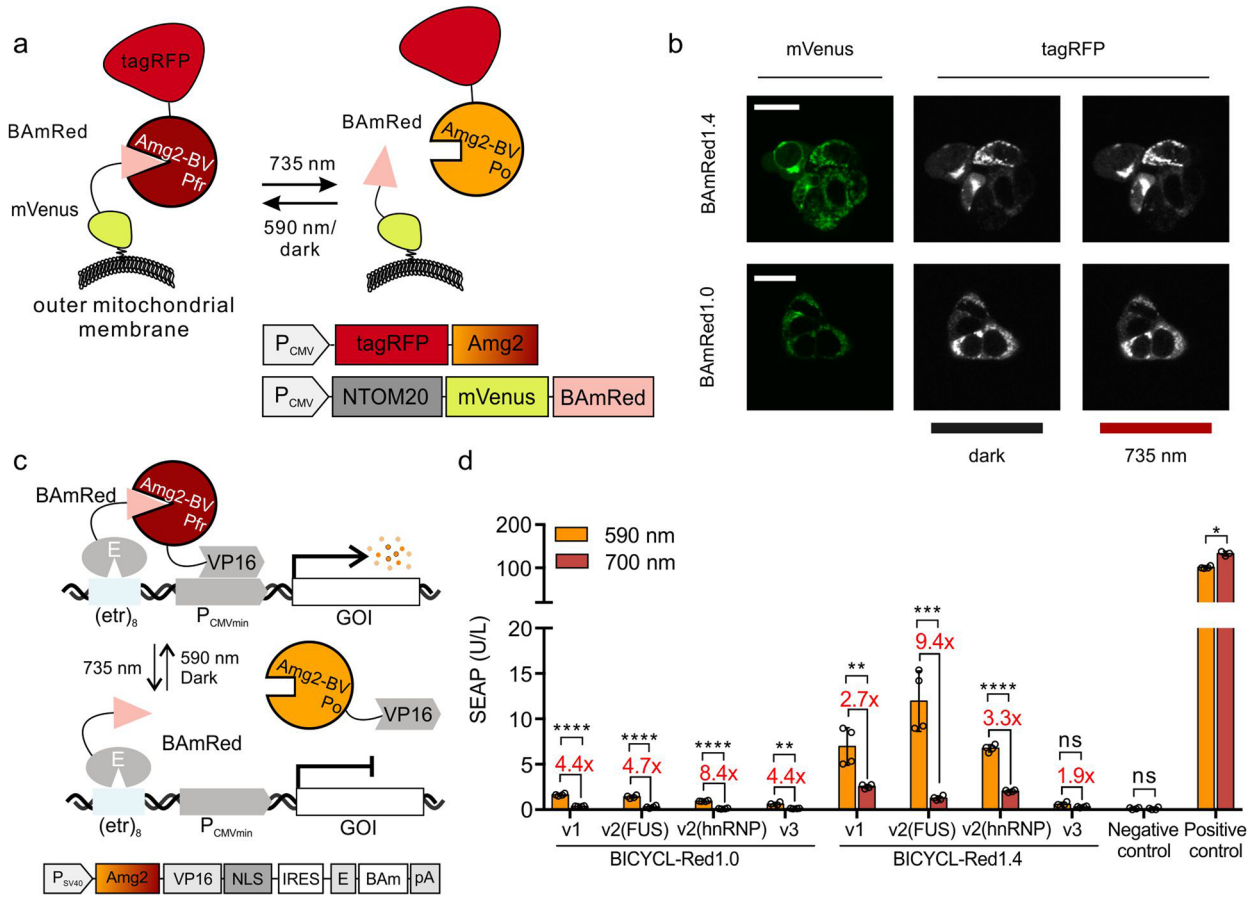

Extended Data Fig. 1 | Performance of the BICYCL system with biliverdin (BV). (a) Schematic showing mVenus-BAmRed anchored to the mitochondrial membrane via an NTOM20 tag. tagRFP-Amg2-BV is localized to the mitochondria in the dark and dispersed in the cytoplasm under far-red light. **(b)** mVenus fluorescence and tagRFP fluorescence confocal microscopy images of Amg2-tagRFP in HEK293T cells with 40 µM biliverdin added 24 h prior to imaging (direct fluorescence of BV could not be detected, as reported by Fushimi *et al.*[17]). Confocal images were obtained on cells co-transfected with pLL-tagRFP-Amg2 and NTOM20-mVenus-BAmRed1.4 (top) or BAmRed1.0 (bottom). (Scale bar: 20 µm). Cells were adapted to the dark state for 30 min prior to acquiring Pfr state images. The experiment was independently repeated four times with similar results. **(c)** Schematic of BICYCL-controlled gene expression with biliverdin. **(d)** Constructs tested for gene expression. CHO-K1 cells were transiently co-transfected with BICYCLs and the SEAP reporter. Cells were exposed to either 590 nm (20 µmol m^{-2} s^{-1}), or 700 nm (20 µmol m^{-2} s^{-1}) for 24 h. Data represent mean values ± SD; n = 3 independent samples. *p* values shown were calculated by 2-tailed unpaired t-test. *$p < 0.0332$, **$p < 0.0021$, ***$p < 0.0002$, ****$p < 0.0001$; n.s., not significant. Source data are provided as a Source Data file. For plasmids and abbreviations, see Supplementary Table 2.

nature research

Corresponding author(s): Andrew Woolley, Maruti Uppalapati, Matias Zurbriggen

Last updated by author(s): Nov 28, 2022

Reporting Summary

Nature Research wishes to improve the reproducibility of the work that we publish. This form provides structure for consistency and transparency in reporting. For further information on Nature Research policies, see our Editorial Policies and the Editorial Policy Checklist.

Statistics

For all statistical analyses, confirm that the following items are present in the figure legend, table legend, main text, or Methods section.

n/a	Confirmed	
☐	☒	The exact sample size (*n*) for each experimental group/condition, given as a discrete number and unit of measurement
☐	☒	A statement on whether measurements were taken from distinct samples or whether the same sample was measured repeatedly
☐	☒	The statistical test(s) used AND whether they are one- or two-sided *Only common tests should be described solely by name; describe more complex techniques in the Methods section.*
☒	☐	A description of all covariates tested
☐	☒	A description of any assumptions or corrections, such as tests of normality and adjustment for multiple comparisons
☐	☒	A full description of the statistical parameters including central tendency (e.g. means) or other basic estimates (e.g. regression coefficient) AND variation (e.g. standard deviation) or associated estimates of uncertainty (e.g. confidence intervals)
☐	☒	For null hypothesis testing, the test statistic (e.g. *F*, *t*, *r*) with confidence intervals, effect sizes, degrees of freedom and *P* value noted *Give P values as exact values whenever suitable.*
☒	☐	For Bayesian analysis, information on the choice of priors and Markov chain Monte Carlo settings
☒	☐	For hierarchical and complex designs, identification of the appropriate level for tests and full reporting of outcomes
☒	☐	Estimates of effect sizes (e.g. Cohen's *d*, Pearson's *r*), indicating how they were calculated

Our web collection on statistics for biologists contains articles on many of the points above.

Software and code

Policy information about availability of computer code

Data collection	For UV-vis analysis, UV WinLab (ver. 2.85.04) Software was used for acquisition. For experiments measuring yeast two hybrid bgal signals, MARS Data Analysis software (BMG labtech) was used for acquisition. For absorbance measurement for phage ELISAs, Gen5 software was used for acquisition. For size exclusion chromatography experiments, BioLogic DuoFlow Version 5.0 was used. For fluorescence measurements, MARS Data Analysis software 3.33 (BMG labtech) was used. For ITC, VPViewer2000 Ver: 1.30.0 was used for acquiring data. For live-cell imaging and photomask experiments, Nikon NIS-Elements AR5.11.03 was used. For quantification of reporter gene expression (Figs. 2e,f; 3e,f; 4b,c; 5g; Extended Fig.1d; Supplementary Fig. 15b,c; 16; 22a; 26 and 27) , the software used for acquisition in the plate reader is MikroWin (version5.18, Berthold) and MARS Data Analysis (version 3.31, BMG Labtech). For RT-qPCR (Supplementary Fig.17, 20 and 21b), the software used for acquisition is Applied Biosystems® Real-Time PCR Software and qPCRsoft4.1(Analytik-Jena).
Data analysis	All data analysis, graph display, and statistics of reporter gene expression were performed with GraphPad (version 3.31) software. The raw data of RT-qPCR experiments were analyzed by the LinRegPCR (2020.2) program. The analysis of DNA sequences and the construction of plasmid maps were performed with Geneious(9.1.8) and Benchling. The composition of microscopy Figures was performed with ImageJ (ver. 1.53a) and OMERO. Mitochondrial-to-cytoplasmic ratio quantification was done with ImageJ (ver. 1.53a). For the analysis of ITC data, NITPIC (ver. 1.2.7) and SEDPHAT/ITCsy (ver. 1.0a) were used.

For manuscripts utilizing custom algorithms or software that are central to the research but not yet described in published literature, software must be made available to editors and reviewers. We strongly encourage code deposition in a community repository (e.g. GitHub). See the Nature Research guidelines for submitting code & software for further information.

Data

Policy information about availability of data

All manuscripts must include a data availability statement. This statement should provide the following information, where applicable:

- Accession codes, unique identifiers, or web links for publicly available datasets
- A list of figures that have associated raw data
- A description of any restrictions on data availability

Source data for the figures are available (Source Data .xls files). The raw and associated data that support the findings of this study is available from the corresponding author upon request. The plasmids used in the experiments of this study will be available on Addgene. The plasmid maps at the public repository JBEI-ICE (https://public-registry.jbei.org).

Field-specific reporting

Please select the one below that is the best fit for your research. If you are not sure, read the appropriate sections before making your selection.

☒ Life sciences ☐ Behavioural & social sciences ☐ Ecological, evolutionary & environmental sciences

For a reference copy of the document with all sections, see nature.com/documents/nr-reporting-summary-flat.pdf

Life sciences study design

All studies must disclose on these points even when the disclosure is negative.

Sample size	The sample size was determined based on our experience of optogenetic experimental setups, and the exact sizes(n) are provided in each figure legends. (references: Nat Methods. 2020 Jul;17(7):717-725. and Nat Biotechnol. 2022 Feb;40(2):262-272.) Screening of hit clones using phage ELISA (Fig. 1c,d) and yeast two hybrid (Fig. 1f), each single clone was inoculated and either screened for binding/beta-galactosidase expression. One replicate (n=1) was performed as this was a screening process to search for mutants that were worth carrying forward with in vitro characterization. Isothermal titration calorimetry (Fig. 1g-i, Fig. S5a-c) and size exclusion chromatography (Fig. S4) for the validation of in vitro binding as well as absorbance measurements of Amg2 were performed once for each BAm binding protein. Yeast two hybrid experiments for validation of BAm binders were done with at least four cultures with each light conditions, consistent with previous optogenetic tools tested in yeast two hybrid settings. see ref. 4 (Hallet, R. A. et al.) in the main text. Measurement of Amg2 fluorescence (Fig. S6a) was done four times on the same sample and averaged. Amg2 fluorescence experiments for measuring binding affinity of BAmRed binding proteins (Fig. S6b-d) were performed in quadruplicate. Measurement of Amg2 dark reversion rates in vitro was performed once (Figure S18). Gene expression experiments where reporters (absorbance of SEAP activities and luminescence of FLuc or GLuc) were measured in CHO-K1 cells. Three distinct wells were taken for each light condition and/or time point. (Fig. 2e,f; 3e,f; 4b,c; 5g; Extended Fig.1d; Supplementary Fig. 15b,c; 16; 22a; 26 and 27) Transcript/mRNA quantifications (Supplementary Fig.17, 21 and 22b): for each illumination/time condition, cell samples were taken, RNA extracted and cDNA generated. For each sample, three technical replicates were used for the quantification of each transcript (Amg2, BAms, SEAP, and GAPDH). Fluorescence microscopy determinations in HEK293T cells (Figs. 2,3,4 and Supplementary Fig. S7-14, S19, 20, 24, 25): 2-4 independent experiments for each construct combination and illumination condition were used for microscopy observation. Images (n shown in the figure legends) were taken with a Nikon microscope for each condition. Representative images are shown. Fluorescence microscopy determinations in photomask (Fig. 4g and Supplementary Fig. 23): 2-3 independent experiments for each combination and illumination condition were used for microscopy observation. Images were taken with a Nikon microscope for each condition. Representative images are shown.
Data exclusions	Outliers in MCR measurements were excluded, but shown in the box plots. Otherwise, no data was excluded.
Replication	All cellular experimental data shown was produced experimentally in at least two independent experiments (different biological material, plasmids, cells). Data shown are representative. All attempts at replication were successful. In vitro experiments involving purified Amg2 protein and screening binding proteins were performed once.
Randomization	Not relevant to our study as the operator cannot influence the outcome of the measurement.
Blinding	No blinding was carried out as the experiments were designed to test under different conditions, i.e. illumination treatments, times, transfection batches, etc. For example, different illumination conditions and times cannot be blinded.

Reporting for specific materials, systems and methods

We require information from authors about some types of materials, experimental systems and methods used in many studies. Here, indicate whether each material, system or method listed is relevant to your study. If you are not sure if a list item applies to your research, read the appropriate section before selecting a response.

Materials & experimental systems

n/a	Involved in the study
☒	☐ Antibodies
☐	☒ Eukaryotic cell lines
☒	☐ Palaeontology and archaeology
☒	☐ Animals and other organisms
☒	☐ Human research participants
☒	☐ Clinical data
☒	☐ Dual use research of concern

Methods

n/a	Involved in the study
☒	☐ ChIP-seq
☒	☐ Flow cytometry
☒	☐ MRI-based neuroimaging

Eukaryotic cell lines

Policy information about cell lines

Cell line source(s)	HEK-293T, Human embryonic kidney, epithelial and adherent cells was a gift from Prof. Allison McGuigan. CHO-K1, Chinese hamster ovary, fibroblastoid and adherent cells. Stable cell lines were generate into CHO-K1 cells.
Authentication	Cell line information can find: American Type Culture Collection (ATCC), www.atcc.org German Collection of Microorganisms and Cell Cultures (DSMZ), www.dsmz.de Cell lines were authenticated by ATCC and DSMZ, not by us.
Mycoplasma contamination	All cell lines were tested monthly for mycoplasma contamination. Mycoplasma contamination of HEK293T cells are tested monthly by the Allison McGuigan lab. No mycoplasma contamination was detected.
Commonly misidentified lines (See ICLAC register)	No commonly misidentified cell lines were used in this study.